Article

Not peer-reviewed version

Structure-Property Relationship in Isotactic Polypropylene Under Contrasting Processing Conditions

Edin Suljovrujic *, Dejan Milicevic, Katarina Djordjevic, Zorana Rogic Miladinovic, Georgi Stamboliev, Slobodanka Galovic *

Posted Date: 12 May 2025

doi: 10.20944/preprints202505.0754.v1

Keywords: Semicrystalline polymers; Polypropylene; Processing conditions; Crystallization; Polymorphism

 doi:10.20944/preprints202505.0754.v1

Article

Structure-Property Relationship in Isotactic Polypropylene Under Contrasting Processing Conditions

Edin Suljovrujic [1,*], Dejan Milicevic [1], Katarina Djordjevic [1], Zorana Rogic Miladinovic [1], Georgi Stamboliev [1,2] and Slobodanka Galovic [1,*]

[1] Vinca Institute of Nuclear Sciences-National Institute of the Republic of Serbia, University of Belgrade, Belgrade, Serbia
[2] Global Supply Line, Adelaide, Australia
* Correspondence: edin@vinca.rs (E.S.); bobagal@vinca.rs (S.G.); Tel. +381113408307

Abstract: Polypropylene (PP), owing to its favorable physical, thermal and mechanical properties, and excellent processability, has become one of the most widely used synthetic polymers. It is known that the overall properties of semicrystalline polymers, including PP, are governed by the morphology, which is influenced by the crystallization behavior of the polymer under particular conditions. Among various types of polypropylene, isotactic polypropylene (iPP) remains the most significant for the industry and has been extensively studied for its polymorphic nature and crystallization behavior over the past five decades. Due to its regular chain configuration, iPP belongs to the group of polymers with a high tendency for crystallization. The rapid quenching of molten iPP fails to produce a totally amorphous polymer, but rather leads to an intermediate crystalline order. In contrast, the slow cooling yields a material with high crystalline content. The processing conditions that occur in practice and industry typically lie between these two extremes and, in some cases, approach either limit. Therefore, the investigation of limits in processability and extreme preparation conditions on morphology, structure, thermal, and mechanical properties can be of great importance, and is the main focus of this research. Two sets of samples were prepared: the first set was obtained by rapid quenching (Qs samples), and the second by very slow cooling from the melt to room temperature (SCs samples). Characterization of samples was performed by optical microscopy (OM), scanning electron microscopy (SEM), wide angle X-ray diffraction (WAXD), Fourier transform infrared spectroscopy (FTIR), differential scanning calorimetry (DSC), dynamic dielectric spectroscopy (DDS), and mechanical measurements. The obtained results were analyzed and discussed in depth, thus providing a detailed insight into the structure-property relationship.

Keywords: semicrystalline polymers; polypropylene; processing conditions; crystallization; polymorphism

1. Introduction

More than 50% of the thermoplastic polymers used in the industry are semicrystalline (consisting of two phases, crystalline and amorphous), making crystallization part of the material and component design process for these materials (Mileva et al., 2018). Crystallization and the presence of a crystalline phase play critical roles in the microstructure, properties (optical, thermal, mechanical, etc.), and long-term stability (Amer et al., 2015; Moore, 1996). PP is probably one of the best examples of how significant the presence of a crystalline phase is, owing to the large difference between atactic PP (aPP), amorphous due to lack of any regularity, which prevents it from crystallization, and semicrystalline ones, which have more regularity and presence of a crystalline phase. The regularity in the configuration of successive stereo centers determines the overall order

 doi:10.20944/preprints202505.0754.v1

(tacticity) of the polymer chain; the carbon atom carrying the substituent (a methyl group) is a stereogenic center in the case of PP. Strictly speaking, the presence of a crystalline phase in the case of PP is directly related to the tacticity of the basic chain structure. The term "tacticity" describes for PP how the methyl (-CH_3) group is oriented in the polymer chain, and it is usually given in percent, using the isotactic index. PP has three possible stereochemical configurations: atactic (aPP, without any regular order, in which case the methyl groups (-CH_3) are randomly aligned), syndiotactic (sPP, with methyls on alternating sides of the chain), and isotactic iPP, with all methyl groups (-CH_3) on the same side of the chain (Ozzetti et al., 2002). An increase in isotacticity leads to a semicrystalline PP with significant crystallinity and favorable thermal and mechanical properties (Arranz-Andrés et al., 2007; Cheng et al., 1991; Paukkeri and Lehtinen, 1993a; Paukkeri and Lehtinen, 1993b). Mechanical properties of PP, such as softening point, rigidity, Young's modulus, strength, and toughness, are improved by increasing isotacticity (Fukuda et al., 2023; Pasquini, 2005; Yamada et al., 1998); the higher the isotacticity (i.e., the isotactic fraction), the greater the crystallinity, and thus also the mechanical properties (Tripathi, 2001). Thus, in contrast to amorphous PP (aPP), which is tacky and rubber-like at room temperature, an increase in isotacticity leads to semicrystalline PPs with favorable mechanical, thermal, as well as most other properties. Therefore, the most important commercial PPs used in industry are isotactic ones (Addeo, 2005; Ariff et al., 2012; Maddah, 2016), with an isotacticity greater than 95% in many cases (Fukuda et al., 2023), and with degree of crystallinity that in industrial products can be up to 60% (Maddah, 2016; Suljovrujic et al., 2024).

Due to its large structural complexity, the great interest of the scientific community, and the wide range of different industrial applications, isotactic PP (iPP) has been studied extensively for its polymorphic characteristics and crystallization behavior since 1954, when Natta et al. synthesized it for the first time (Natta, 1955). Polymorphic iPP can exist in several crystalline forms (modifications) that differ by the molecular arrangement of the polymer chains, and its crystallization is strongly dependent on crystallization conditions and molecular characteristics. Thus, iPP is unique in adopting the same three-fold helical conformation with a 6.5 Å repeat distance in as many as three distinct crystalline polymorphs: monoclinic (α), hexagonal (β), triclinic (γ), and in the so-called mesomorphic (smectic) phase as well (Bogoeva-Gaceva, 2014; Brückner et al., 1991; Seguela et al., 1999; Shang et al., 2014). In all of the crystal structures, the chain is packed in the lattice as a left or/and right-handed 31-helix conformation with either an 'up' or 'down' position of the methyl groups (Arvidson et al., 2010; Sharaf and Kloczkowski, 2024; Suljovrujic, 2000; van der Meer, 2003). The β-hexagonal or γ-triclinic form may be obtained while crystallizing from the melt at high undercoolings or pressures or with the addition of nucleating agents (Arvidson et al., 2010; Bogoeva-Gaceva, 2014). Thus, the β form is favored by the presence of nucleating agents, temperature gradient, and shear stress, while the γ form is hardly formed under the conditions used in industry and is favored during crystallization under elevated pressure or when the isotactic sequence length is interrupted (De Rosa et al., 2002; Scoti et al., 2023; Sharaf and Kloczkowski, 2024). Rapid quenching of molten iPP fails to produce a completely amorphous polymer but rather leads to a mesomorphic (smectic) form with intermediate crystalline order (Arvidson et al., 2010; Suljovrujic et al., 2010; Vittoria and Perullo, 1986). The mesomorphic phase is arranged roughly as in the α crystal, with defects along the chains and in the packing perpendicular to the chain direction (Auriemma et al., 2005). This form is considered the reason for the transparency in rapidly cooled films (due to low order and small crystallites) and often occurs in industrial processing since the plastic is usually cooled quickly (Mileva et al., 2009; Stupp et al., 1979). Nevertheless, iPP has been shown to crystallize predominately in the thermodynamically most stable monoclinic α-form under isothermal crystallization, in slow cooling and during melt spinning of filaments (Arvidson et al., 2010; Kim et al., 1997; Natta, 1955); this form often occurs in practice, and it is generally characterized by the highest crystallinity among other forms, which can exceed 50% in industrial products.

The crystal structure and crystallization kinetics of iPP are well established (Karger-Kocsis and Bárány, 2019). iPP crystallization is a critical process associated with the arrangement of three-fold helical molecular chains. It was found that tacticity notably influenced the rate of nuclei seeding,

 doi:10.20944/preprints202505.0754.v1

where the high-tacticity iPP sample exhibited a faster nucleation rate (Rungswang et al., 2019). However, at the nm scale (in most cases between 5-25 nm), the chains are arranged in the lamella, and the most common crystalline structures under melt processing conditions are lamellar-like crystallites (Bassett and Olley, 1984). At a larger (μm) scale, initial nuclei by propagation and multiplication of lamellae lead to spherically symmetric superstructures, i.e., spherulites (Ryan et al., 1997). The structure of spherulite was established by the pioneer work of Bassett and co-workers, where the notions of dominant and subsidiary lamellae were introduced, and further investigated with a combination of light-microscope methods, etching method and electronic microscope (EM), and atomic force microscope (AFM) (Bassett, 1981; Bassett et al., 1963; Bassett and Olley, 1984; Bassett and Vaughan, 1985; Chan and Li, 2005; Cong et al., 2012; Jiang et al., 2025; Michaeli et al., 2001; Park et al., 2001; Raimo and Silvestre, 2009; Schönherr et al., 1993; Yang et al., 2023; Zhou et al., 2005; Zhou et al., 2017). In broadest generality, a spherulite can be defined as a crystal aggregate having spherical symmetry and which arises by radial growth of crystals (stacked lamellae) from a common center (Imai and Kaji, 2006; Rungswang et al., 2019). According to Norton, such growth and the resulting spherically symmetrical end product, however, can arise in more than one way, most conveniently classified into two main categories: central multidirectional growth and sheaf-like unidirectional growth (Norton and Keller, 1985). Depending on crystallization conditions, four different types of spherulites can be observed (Norton and Keller, 1985; Padden and Keith, 1959; Park et al., 2001; Stachurski and Macnicol, 1998; Zhou et al., 2017); detailed descriptions of these structures, their characteristics and conditions of formation are beyond the scope of this paper. The simplest morphological model of semicrystalline polymers is a two-phase model composed of crystalline and amorphous structures. However, between the pure amorphous (also known as mobile amorphous fraction - MAF) and crystalline regions (lamellas and spherulites), the intermediate phase can be distinguished; this interphase is also known in literature as rigid-amorphous fraction (RAF) or disordered crystalline phase (Androsch et al., 2010; Di Lorenzo and Righetti, 2018; Kida and Yamaguchi, 2022; Schawe, 2017; Sharaf and Kloczkowski, 2024; Zia et al., 2008). The polymer chains in the interphase region are restricted in their movement by the more ordered crystal phase and consist of the fold surface of the lamellae, chain loops, entanglements, knots, tie chains, and chain cilia (Androsch et al., 2010; Zuo et al., 2007). While the molecular mobility of chains in MAF, which are liquid-like amorphous chains, is released at the glass transition temperature, the molecular motion of chains in RAF is constrained at T_g because of strong coupling with the crystalline structure (Kida and Yamaguchi, 2022).

Therefore, crystallization kinetics is of paramount importance when designing a polymer for specific applications to obtain the desired properties from the morphology developed during solidification. For polymer-based materials, including neat polymers, blends, composites, and hybrids, processing is crucial for linking polymer materials' physical/chemical properties to their practical applications. By adopting widespread melt processing techniques, such as extrusion, heat compression, film stretching/blowing, injection molding, and fiber spinning, distinctly different temperature and/or stress fields may be imposed on the melts of semicrystalline polymeric materials, leading to tremendous differences in the microscopic structures, crystallinity and macroscopic properties of the final products (Chen et al., 2020; Sigalas et al., 2023). A good example is commercial PP (which is isotactic mainly); even with unchanged chemical composition and molecular chain architecture, iPP can exhibit a wide range of final microstructures, different crystal architectures, and, consequently, large variations in macroscopic properties. Therefore, variation in processing conditions after melting implies how to produce superior performance (Hine et al., 2005; Laura et al., 2003) and/or functionalization (Haggenmueller et al., 2007; Tangirala et al., 2004) of the final products, but also how the same grade polymer can be suitable for different applications by tuning processing conditions. Processing conditions after melting, such as cooling rate and/or solidification temperature, play a significant role in obtaining isotropic polymeric structures. Thus, for iPP, it is well known that in the case of slow cooling rates, the crystalline α-form with a spherulite morphology and a large content of crystalline phase (high crystallinity) is typical. In contrast, by quenching at

 doi:10.20944/preprints202505.0754.v1

room temperature, or as it is better at much lower temperatures, or/and by rapid cooling of molten PP at a rate of more than 10^2 to 10^3 K/s, mesomorphic (smectic) phase can be obtained (Androsch et al., 2010; Brucato et al., 2002; De Rosa et al., 2017; Dudić, 2002; Jiang et al., 2016; Mollova et al., 2013). The mesomorphic phase has molecular ordering between that of the amorphous and of the true crystalline phase (Androsch et al., 2010; Fu et al., 2019; Hendra et al., 1984; Konishi et al., 2005), with molecules arranged roughly as in the α crystal (Androsch et al., 2010), but containing defects along the chains and in the packing perpendicular to the chain direction (Auriemma et al., 2005; Ferrero et al., 2000). The effect of isotacticity on the mesomorphic phase-forming properties was investigated by Konishi et al. (Konishi et al., 2005); under the same quenching conditions, iPP having higher isotacticity formed the mesomorphic phase, while iPP having lower isotacticity did not form the mesomorphic phase but the α-crystalline form. Nevertheless, according to the same author, the structure of the mesomorphic phase is still an open question. While most researchers assign the structure to the smectic phase, additional explanations are based on crystal defects: paracrystalline, conformational disorder (condis) crystal, and micro- or nanocrystal (Konishi et al., 2005). The mesophase structure can be transformed into the α-form with a nodular morphology by annealing at temperatures above 60 °C due to the ordering of the lateral direction of molecular chains (Androsch et al., 2010; Di Sacco et al., 2021; Dudic et al., 2002; Fu et al., 2019; Jiang et al., 2016; Nitta and Odaka, 2009; Zia et al., 2009). The lamellar structure of the α-form crystals prepared from the mesophase only comprises the parent lamellar crystals (Pasquini, 2005). The mechanism by which the meso-to-α phase transformation takes place has been investigated, and it has been reported that left- and right-handed helices occur during the annealing process (Androsch, 2008; Miller, 1960). The mesomorphic (smectic) to the α monoclinic phase transformation upon heating is possibly by thickening of existing α crystals and/or by structural rearrangements in the mesomorphic phase (Martorana et al., 1999); the mechanism of this structural rearrangement has yet to be determined in any conclusive way (Androsch, 2008; Arvidson et al., 2010; Gomez et al., 1987; Hanna et al., 1988; Konishi et al., 2006; Zia et al., 2006). Since the formation of RAF is evidenced for both mesomorphic and crystalline iPP, structural changes of the RAF seem to be very important for understanding the crystallization of mesophase (Fu et al., 2019; Zia et al., 2008; Zia et al., 2009).

Processing conditions combined with specific structural characteristics can lead to products with large differences in final microstructure, crystallinity, and properties despite the starting material being the same. Thus, this work aims to shed some new light on the investigation of the influence of processing conditions on the crystalline architecture and final properties of commercial PPs. Two opposite cooling procedures after compression molding, rapid quenching and slow cooling, which represent border conditions in the case of industrial processing, were applied to obtain PP samples with great diversity in microstructure and properties. Microstructures and crystalline architectures were studied by optical microscopy (OM), scanning electron microscopy (SEM), Fourier transform infrared spectroscopy (FTIR), and wide angle X-ray diffraction (WAXD). Differential scanning calorimetry (DSC) was used to study the thermal properties. For the first time, dynamic dielectric spectroscopy (DDS) is used to study the difference in molecular mobility in the iPP mesomorphic (smectic) and α-monoclinic phases. Special attention was focused on tensile properties and stress-relaxation behavior to gain profound insight into the relationship between structure and mechanical properties. Two additional PPs (one with nucleating and antistatic agents and the other with ionizing radiation stabilizers) are used in mechanical measurements to confirm the obtained relations between the revealed mechanical behavior of final structures and applied processing conditions after compression molding. This work also presents a broad discussion of literature data in line with the new observed results presented in this paper.

2. Experimental

2.1. Materials

Two types of PP: PP-A (isotactic PP used in various industries obtained from SIGMA-ALDRICH, with a high index of isotacticity, density ϱ=0.90 g cm^{-3}, M_w=250000, M_n=67000, more information at:

 doi:10.20944/preprints202505.0754.v1

https://www.sigmaaldrich.com) and PP-H (commercial PP HIPOLEN MA2CR intended for the production of goods for pharmaceuticals, cosmetics, and thin-walled containers with an index of isotacticity >95% (≥ 98% according to ISO/DIS 1873-1), ϱ=0.91 g cm^{-3}, M_w=136000, M_w/M_n = 4.95, more information at: https://hipol.com) were thoroughly examined. In an attempt to get a more complete picture of the influence of different preparation methods on the mechanical properties, two additional commercial PPs were tested, one with nucleating and antistatic agents and the other containing stabilizers against ionizing radiation. The first one is PP-T (TIPPLEN H 949 is a high melt flow PP homopolymer with outstanding processability for shorter cycle times, which contains nucleating and antistatic agents. Melt flow rate: 45 g/10 min, ϱ=0.90 g cm^{-3}, more information at: https://molgroupchemicals.com). The second one is PP-P (PP-PURELL HP 371P with a gamma ray stabilizing additivation for injection molding applications, primarily designed for disposable syringes for medical applications; Melt flow rate: 18 g/10 min, ϱ=0.90 g cm^{-3}, more information at: https://www.matweb.com).

Isotropic sheets were prepared by compression molding for 8 minutes in a Carver laboratory press at 190 °C and gradual pressure increment up to 3.28 MPa. The first set of samples (Qs samples) was obtained by quenching in the ice-water mixture; the use of ice-water-quenched PP is recommended when increased transparency, impact strength, and flexibility are desired (Stupp et al., 1979). The second set was prepared by slow cooling from the melt to room temperature, keeping the samples between the press platens (SCs samples). Subsequently, PP samples of different sizes (depending on the type of measurement) were cut from the obtained isotropic foils, 0.28 ± 0.02 mm thick, and used further.

2.2. Measurements

Microstructure characterization was performed by the Carl Zeiss "AxioImager A1" optical microscope and the JSM 5300 scanning electron microscope. OM photomicrographs were captured and analyzed by the high-resolution microscopy camera (AxioCam, Carl Zeiss) and the image processing software (AxioVision, Carl Zeiss). For SEM analyses, the surface of the samples was covered with a 10 nm thick layer of gold using a Polaron E5200 sputter coater. The obtained thickness was verified by profilometric measurements (Suljovrujic et al., 2021).

Fourier Transform Infrared spectroscopy of PP films was performed in the attenuated total reflectance mode (ATR-FTIR). The spectra were recorded using a Nicolet 6700 spectrometer (Thermo Scientific) at room temperature in the wavenumber range of 4000–400 cm^{-1} with a resolution of 4 cm^{-1}. The spectra are the averaged values of three identically prepared samples randomly selected. A procedure for the determination of crystal fraction (crystallinity) is performed in accordance with analyses done by the Lanyi equation (Lanyi et al., 2018, 2020).

WAXD analyses were made by a Philips PW 1710 diffractometer. The data were collected in the 2θ =5°-90° range, with a step length of 0.03° and an exposure time of 4s per step. The average out-of-plane crystallite size of the PPs (L) was estimated from the (110) reflections using the Scherrer equation: $L = K \lambda/\beta \cos\theta$, where λ is the wavelength of CuK_α radiation (λ = 1.5418 Å), θ corresponds to the Bragg angle, β is the full width at half maximum (FWHM) in radians, K is the coefficient taken to be 0.89. The deconvolution of the X-ray diffractograms was performed using a Gaussian-Lorentzian-pseudo-Voigt asymmetric function to separate the amorphous (A_{am}) and the crystalline (A_c) content and calculate the crystallinity, crystallite size, and the space between the structural layers. According to the profile fitting process, the share of the crystalline fraction was calculated as $\chi_c=A_c/(A_c+ A_{am})x100\%$ (Tarani et al., 2023).

For the differential scanning calorimetry (DSC) measurements, a Perkin Elmer DSC-4 was used. Samples of 7-8 mg were analyzed by heating from 320 to 470 K at a rate of 10 K/min, and the peak melting temperature (T_m), FWHM (full width at half maximum), melting enthalpies (ΔH_m), and crystallinity (χ) were derived from the heating scans. The degree of crystallinity was calculated using ΔH_f=209 J/g as the heat of fusion of a perfectly (100 %) crystalline PP. In the case of PP samples with mesomorphic (smectic) phase, besides the enthalpy of melting (ΔH_m), we also determined cold

 doi:10.20944/preprints202505.0754.v1

crystallization (ΔH_c), while the degree of crystallinity (χ) was calculated according to $\chi = (\Delta H_m - \Delta H_c)/\Delta H_f$ equation. DSC measurements were performed on five identically prepared samples of each kind, randomly selected. The presented results are averaged values.

Dielectric spectra of the samples in the form of discs, 1.3 cm in diameter, were measured on Agilent 4284A Precision LCR Meter coupled with a 22C-kriodin(R) cryo-system, as a function of temperature (20-410 K) and in the frequency range 10^2-10^6 Hz. Dielectric measurements were taken at increments of approximately 2 K, with a heating rate of 0.5 K/min between equilibrated temperatures. At each equilibrated temperature, capacitance and tanδ measurements were taken at 24 frequencies, emphasizing 100 kHz and 1 MHz.

Tensile properties were measured using Shimadzu AGS-10kN. Dumbbell-shaped specimens were cut from differently prepared, 0.28 mm thick, PP films using a cutter and had a gauge length of 30 mm and a width of 4 mm. The unexposed and irradiated samples were elongated at room temperature (25 °C) with a constant elongation rate of 20 mm/min. The tensile stress was determined by dividing the tensile load by the initial cross-section, and the tensile strain was calculated from the ratio of the increment of the length between clamps to the initial gauge length. Young's modulus was evaluated from the initial slope. The reported values of the investigated mechanical parameters are averages of the values obtained from the 20 tensile bars of each material. Namely, out of 24 initial values, the two biggest and two smallest ones were excluded.

Fourier Transform Infrared spectroscopy of PP films was performed in the attenuated total reflectance mode (ATR-FTIR). The spectra were recorded using a Nicolet 6700 spectrometer (Thermo Scientific) at room temperature in the wavenumber range of 4000–400 cm^{-1} with a resolution of 4 cm^{-1}. The spectra are the averaged values of three identically prepared samples randomly selected. A procedure for the determination of crystal fraction (crystallinity) is performed in accordance with analyses done by the Lanyi equation (Lanyi et al., 2018, 2020).

WAXD analyses were made by a Philips PW 1710 diffractometer. The data were collected in the 2θ =5°-90° range, with a step length of 0.03° and an exposure time of 4s per step. The average out-of-plane crystallite size of the PPs (L) was estimated from the (110) reflections using the Scherrer equation: $L = K\,\lambda/\beta\cos\theta$, where λ is the wavelength of CuK$_\alpha$ radiation (λ = 1.5418 Å), θ corresponds to the Bragg angle, β is the full width at half maximum (FWHM) in radians, K is the coefficient taken to be 0.89. The deconvolution of the X-ray diffractograms was performed using a Gaussian-Lorentzian-pseudo-Voigt asymmetric function to separate the amorphous (A_{am}) and the crystalline (A_c) content and calculate the crystallinity, crystallite size, and the space between the structural layers. According to the profile fitting process, the share of the crystalline fraction was calculated as $\chi_c = A_c/(A_c + A_{am})$x100% (Tarani et al., 2023).

For the differential scanning calorimetry (DSC) measurements, a Perkin Elmer DSC-4 was used. Samples of 7-8 mg were analyzed by heating from 320 to 470 K at a rate of 10 K/min, and the peak melting temperature (T_m), FWHM (full width at half maximum), melting enthalpies (ΔH_m), and crystallinity (χ) were derived from the heating scans. The degree of crystallinity was calculated using ΔH_f=209 J/g as the heat of fusion of a perfectly (100 %) crystalline PP. In the case of PP samples with mesomorphic (smectic) phase, besides the enthalpy of melting (ΔH_m), we also determined cold crystallization (ΔH_c), while the degree of crystallinity (χ) was calculated according to $\chi = (\Delta H_m - \Delta H_c)/\Delta H_f$ equation. DSC measurements were performed on five identically prepared samples of each kind, randomly selected. The presented results are averaged values.

Dielectric spectra of the samples in the form of discs, 1.3 cm in diameter, were measured on Agilent 4284A Precision LCR Meter coupled with a 22C-kriodin(R) cryo-system, as a function of temperature (20-410 K) and in the frequency range 10^2-10^6 Hz. Dielectric measurements were taken at increments of approximately 2 K, with a heating rate of 0.5 K/min between equilibrated temperatures. At each equilibrated temperature, capacitance and tanδ measurements were taken at 24 frequencies, emphasizing 100 kHz and 1 MHz.

Tensile properties were measured using Shimadzu AGS-10 kN. Dumbbell-shaped specimens were cut from differently prepared, 0.28 mm thick, PP films using a cutter and had a gauge length of

 doi:10.20944/preprints202505.0754.v1

30 mm and a width of 4 mm. The unexposed and irradiated samples were elongated at room temperature (25 °C) with a constant elongation rate of 20 mm/min. The tensile stress was determined by dividing the tensile load by the initial cross-section, and the tensile strain was calculated from the ratio of the increment of the length between clamps to the initial gauge length. Young's modulus was evaluated from the initial slope. The reported values of the investigated mechanical parameters are averages of the values obtained from the 20 tensile bars of each material. Namely, out of 24 initial values, the two biggest and two smallest ones were excluded.

3. Results and Discussion

3.1. Microstructure Investigation

Microstructure comparison (with a gradual increase in magnification) of PP-A and PP-H samples obtained by slow cooling (SCs) is presented in Figs. 1a and 1b, respectively. OM images (presented at the top of Figs. 1a and 1b) show spherically symmetric superstructures, i.e., spherulites, among which the largest number are deformed. Significantly larger spherulites ($d > 100$ μm) are visible in the case of PP-H, indicating a higher potential of this material for the formation of large crystalline superstructures. Spherulite surface morphology, spatial boundaries, and defects are more clearly visible from SEM microstructures at intermediate magnifications (up to x 10.000) for both PPs. Higher SEM magnification (Figs. 1c and 1d) also shows the presence of large cavities and fiber-like formations at the spherulite boundaries, which are more pronounced in PP-H. The presence of cavities at crystalline surfaces can be explained by the absorption of material from low density (amorphous) regions during spherulite growth at very slow cooling conditions from the melt. On the other hand, fiber-like formations consisting of bundles of thinner fibers (that can be seen at high magnifications) represent inter-phase regions (RAF or disordered crystalline phase) with restricted mobility, which cannot be inserted into spherulites and contain a large concentration of tie chains, chain loops, etc. In contrast to the investigated PP samples obtained by slow cooling in the case of samples obtained by rapid quenching (Qs), relatively smooth, non-porous surfaces with no signs of noticeable crystalline architecture and defects are visible even at high magnifications (x 100.000). According to Androsch et al. (Androsch et al., 2010), the absence of superstructure architecture (spherulites) due to quenching at rates faster than 10^2 K/s to ambient temperature should be expected.

 doi:10.20944/preprints202505.0754.v1

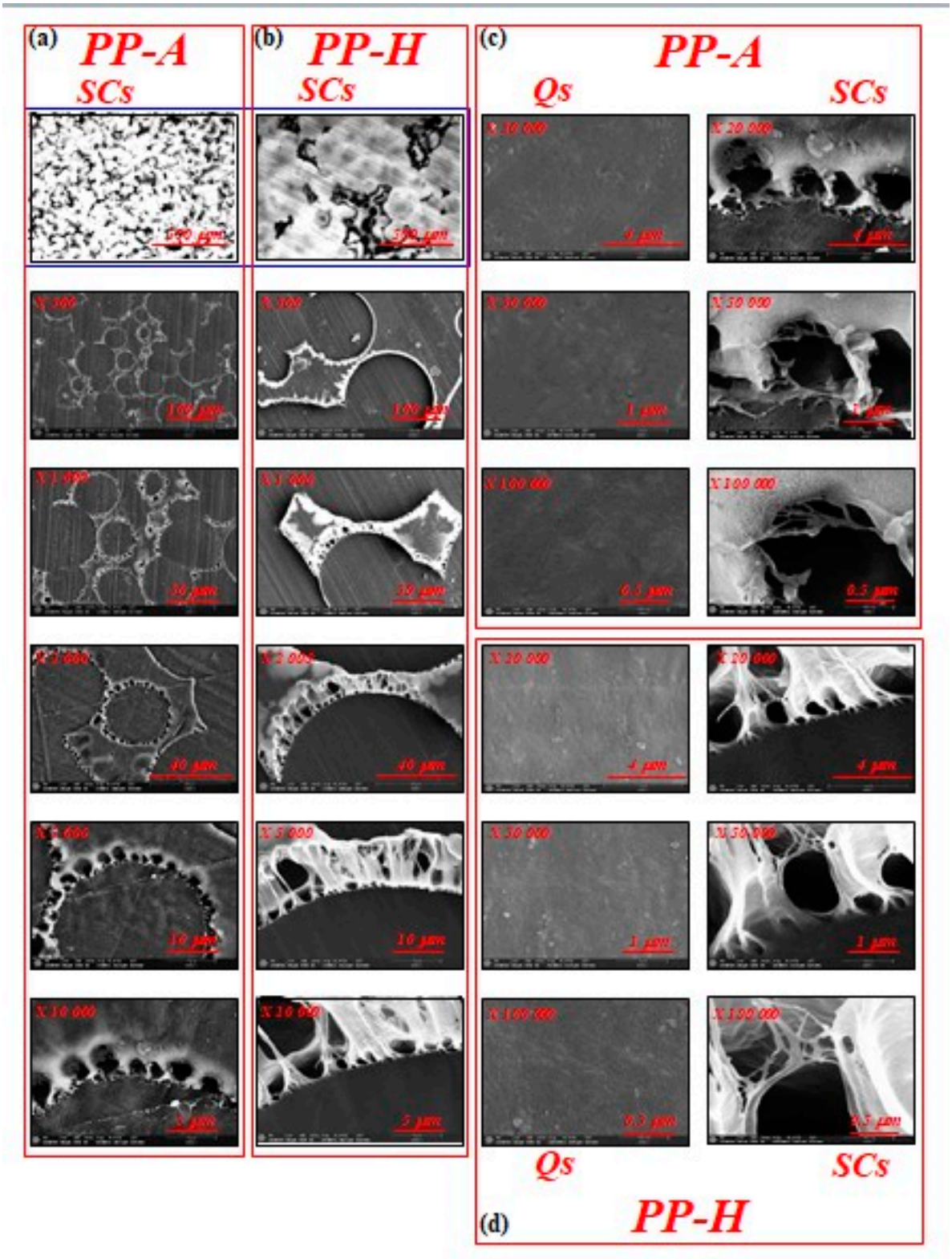

Figure 1. SEM images of *SCs* surfaces for *PP-A* (a) and *PP-H* (b) at different magnifications from x500 up to 10000). The exception to this are the images at the top, which represent ones obtained by OM at magnification x100; SEM images of *Qs* (left) and *SCs* (right) surfaces for *PP-A* (c) and *PP-H* (d) at large magnifications (from x20.000 up to 100000).

3.2. WAXD Study

WAXD patterns of PP-A and PP-H samples obtained after quenching in an ice-water mixture (Qs) and slow cooling from melt to room temperature (SCs) are presented in Figs. 2a and 2b, respectively. A large number of narrow peaks ((110), (040), (130), (111), (131), (041), (060), (150), (200),

 doi:10.20944/preprints202505.0754.v1

(222) reflections) in the SCs diffractograms clearly confirm the presence of highly developed monoclinic (α) form for both PPs (PP-A and PP-H) (Reddy et al., 2009; Stojanović et al., 2005; Zhou et al., 2015). Furthermore, the parameters related to the crystal phase obtained from the SCs diffractograms are determined: PP-A (degree of crystallinity χ=55±1%, crystallite size $L_{(110)}$=17.5 nm) and PP-H (degree of crystallinity χ=56±1%, crystallite size $L_{(110)}$=21.1 nm). This data indicates that significantly larger spherulites in the case of PP-H, obtained previously by comparison of surface microstructures, do not lead to a significant variation in the shape of the diffractogram as well as the overall crystallinity (degree of crystallinity), since the difference is less than 2%. On the other hand, while the difference in crystallinity is relatively small, the crystallite size is about 20% larger in the case of PP-H.

While the slow cooling of different grade commercial PP, as a result, has developed a monoclinic (α) form with high crystallinity, quenching in an ice-water mixture after melting shows significant differences in the obtained diffractograms. Thus, the same applied quenching procedure, in the case of PP-H, results in the clear mesomorphic (smectic) form characterized by two wide diffraction peaks, while in the case of PP-A, it leads to the intermediate form, i.e., a mixture of monoclinic (α) form and mesomorphic (smectic) one. In diffractograms of Qs PP-A, three peaks can be clearly noticed ((110), (040), (130)), while a broad peak at 21.5 ° corresponds to (111), (131), and (041) reflections. On the other hand, microstructure investigations of PP-A Qs samples indicate the absence of spherulite morphology and microstructure similar to those of mesomorphic (smectic) PP-H. Nevertheless, parameters calculated from the Qs PP-A diffractogram give a degree of crystallinity χ=36±2% with crystallite size $L_{(110)}$=9.5 nm. Rapid quenching of molten PP-H fails to produce a totally amorphous polymer, but rather leads to a mesomorphic (smectic) form. Although the X-ray scattering curve for the quench-cooled sample is very similar to that for atactic PP, the presence of a second scattering maximum at 21.3° suggests the existence of a greater degree of order (Caldas et al., 1994); low-order and small crystallites are considered a cause for increased transparency and flexibility in quenched PP with mesomorphic (smectic) form (Stupp et al., 1979). This phase is stable at room temperature for long periods; still, it is very sensitive to thermal treatment, and upon heating, the mesomorphic transforms into the monoclinic form by thickening of existing crystals and/or by structural rearrangements in the mesomorphic (smectic) phase (Arvidson et al., 2010; Cohen and Saraf, 2001; Dudic et al., 2002; Suljovrujic et al., 2010). For Qs PP-H samples, i.e., mesomorphic (smectic) form, it is not easy to determine the parameters related to the crystal phase from the diffractogram; however, calculations indicate that the degree of crystallinity is lower than 30%, while crystallite size $L_{(110)} \leq 3$ nm. Due to the presence of a large number of small crystallites and low crystallinity in mesomorphic (smectic) form and the presence of only two broad peaks in WAXD spectra, it is likely that FTIR and DSC measurements are more suitable for investigation of the crystalline phase.

 doi:10.20944/preprints202505.0754.v1

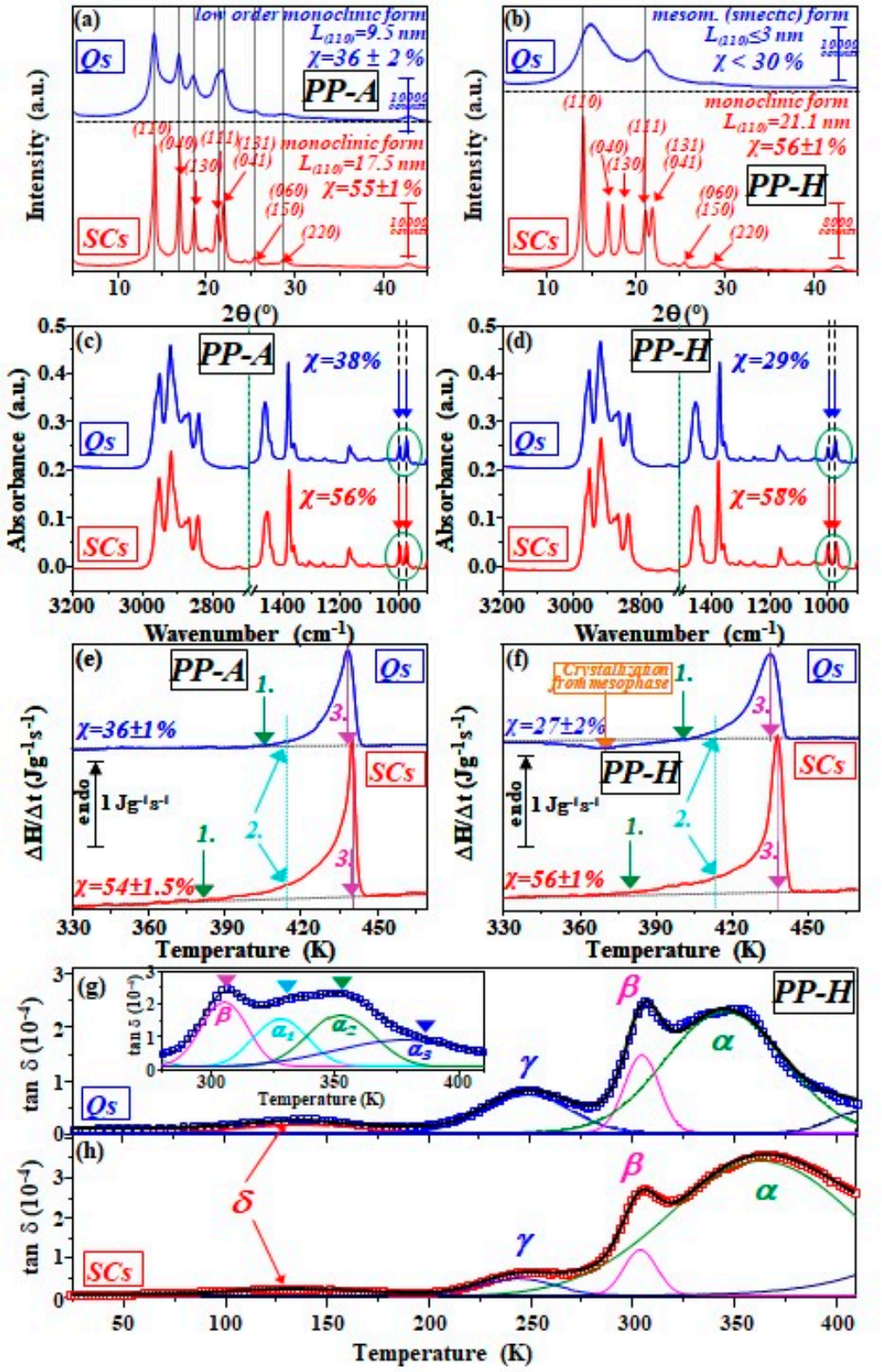

Figure 2. WAXD diffractograms of *Qs* and *SCs* samples for *PP-A* (a) and *PP-H* (b) samples; ATR-FTIR spectra of *Qs* and *SCs* samples for *PP-A* (c) and *PP-H* (d) samples; DSC heating thermograms of *Qs* and *SCs* samples for *PP-A* (e) and *PP-H* (f) samples; Experimental (□) and fitted (solid line) dielectric loss tangent spectra at 1 MHz for *PP-H* samples which are quenched (g) and slowly cooled (h). The insert in Fig. 2g is the dielectric loss tangent spectra of *PP-H* for *Qs* sample in the high temperature α relaxation region.

3.3. ATR-FTIR Spectroscopy

 doi:10.20944/preprints202505.0754.v1

The conformational change of iPP during the crystallization process has been carefully studied by Fourier transform infrared (FTIR) spectroscopy in the past (An et al., 2008; Geng et al., 2009; Konishi et al., 2005; Qian et al., 2021; Reddy et al., 2009; Zhu et al., 2001). Furthermore, it is proposed that tacticity in PP can be determined by FTIR, besides extraction in boiling heptane and ^{13}C-NMR spectroscopy (Kissin, 1985; Luongo, 1960; Ozzetti et al., 2002). With the in situ IR microspectroscopic imaging technique, conformational ordering at the growth front of the spherulite of iPP is also studied during the isothermal crystallization process at different temperatures (Cong et al., 2010; Cong et al., 2012). The mechanism of the meso-to-α transition of iPP and Ethylene–Propylene random copolymers was investigated by FTIR spectroscopy in detail by Di Sacco et al. (Di Sacco et al., 2021). Nevertheless, in this study, the focus is on the calculation of crystallinity from the presented ATR-FTIR spectra (Figs. 2c and 2d) following the Lanyi equation, χ=0.62 h_{998}/h_{973} (where h_{998} and h_{973} are peak heights at 998 and 973 cm^{-1}, respectively) (Lanyi et al., 2018, 2020). Besides Lanyi et al., other comparable approaches for determining the degree of crystallinity via FTIR spectroscopy have already been published by Burfield et al. (Burfield and Loi, 1988), Huy et al. (Huy et al., 2004), and Kilic et al. (Kilic et al., 2016). The peak at 998 cm^{-1} corresponds to the crystalline phase, and the height of this peak, according to literature data, grows linearly with the degree of crystallinity (Burfield and Loi, 1988; Heinen, 1959; Li et al., 2011). The peak at 973 cm^{-1} correlates linearly with the penetration depth of the IR-radiated volume and is independent of the degree of crystallinity (Lamberti and Brucato, 2003; Quynn et al., 1959; Tadokoro et al., 1965). Therefore, the ratio of the maximum peak heights of the peak at 998 cm^{-1} (h_{998}) and 973 cm^{-1} (h_{973}) is considered as a linearly proportional measure of the degree of crystallinity χ with slope 0.62 determined by Lanyi et al. (Lanyi et al., 2018, 2020). Such calculated degrees of crystallinity χ from the presented ATR-FTIR spectra (Figs. 2c and 2d) are for Qs and SCs PP-A samples 38% and 56%, while in the case of PP-H are 29% and 58%, respectively. These data are in very good agreement with those previously obtained by WAXD.

3.4. Calorimetric Study

Besides thermal properties, DSC measurements are also suitable for investigating the crystalline phase of thermoplastic polymers such as PP. DSC heating scans (thermograms) of PP-A and PP-H samples obtained after quenching in an ice-water mixture (Qs) and slow cooling from melt to room temperature (SCs) are presented in Figs. 2e and 2f, respectively. Regardless of the type of PP and applied treatment after melting, the presence of well-resolved endothermic peaks due to the melting of the crystalline phase can be clearly observed for all samples. The existence of a broad exothermic peak can only be seen in the case of PP-H quenched (Qs) samples and can be attributed to crystallization from mesophase, i.e., low-temperature crystallization (into the α-monoclinic phase) of polymer portions that, on the macromolecular scale, are placed close to the initially present smectic crystal phase (Dudić et al., 2002; Milicevic et al., 2012; Milicevic et al., 2007a). This transformation upon heating is by structural rearrangements in the mesomorphic phase and/or thickening of existing α crystals (Martorana et al., 1999), and since it occurs at much lower temperatures than melting, it is also known as a cold crystallization. Therefore, the endothermic peak in PP-H quenched (Qs) samples, which occurs at much higher temperatures due to the melting of the crystalline phase, originates not only from the melting of the smectic crystalline phase, present at room temperature, but also from the crystal portions obtained by crystallization during heating. Following the above, the crystallinity was calculated according to the procedure given in the experimental part. Taking this into account, the degree of crystallinity obtained from DSC measurements is determined for PP-A (χ=54% for SCs and χ=36% for Qs samples) and PP-H (χ=56% for SCs and χ=27% for Qs samples). Comparing these data with that obtained from WAXD and FTIR spectroscopy, a good agreement can be observed in the degree of crystallinity. However, the degree of crystallinity obtained from DSC measurements is calculated using the value ΔH_f=209 J/g as the heat of fusion of a perfectly (100 %) crystalline PP (Brandrup et al., 1999; Wunderlich, 1990). The ΔH_f values reported in the literature can deviate more or less from this value, but in most cases, they are between 150 and 250 J/g (Lanyi et al., 2020). Besides the degree of crystallinity, DSC measurements are used to determine the melting

 doi:10.20944/preprints202505.0754.v1

temperature (T_m) of PP-A (438 K for Qs and 440 K for SCs samples) and PP-H (435 K for Qs and 439 K for SCs samples). The higher values of melting temperatures are revealed in slowly cooled (SCs) samples, i.e., those with fully developed α -monoclinic phase and spherulites, than in the case of quenched (Qs) (that are previously reported), and the obtained results are in good agreement with literature data where T_m ranges from 433 to 439 K (Chang et al., 2017; Fukuda et al., 2023; Seguela et al., 1999). For comparison, perfectly iPP has a slightly higher value (T_m=444 K) while sPP has lower ones (423 K ≤ T_m ≤433 K) (Haftka and Könnecke, 1991; Lee et al., 2003; Rodriguez-Arnold et al., 1994). Nevertheless, the shift to higher melting temperature can be explained by the increase in crystallite size rather than crystallinity (Farrow, 1963; Teodorescu et al., 2024). Namely, in the case of SCs samples, long period of the crystallites (i.e., stacking period, which is usually extremely regular) and lamellar thickening, which are favored by slow cooling after melting, lead to a large increase in crystallite dimension and formation of very thick lamella with higher thermal stability and perfection (Chang et al., 2017; Di Sacco et al., 2021; Guleria et al., 2024; Huang et al., 2019; Ronkay et al., 2020; Tencé-Girault et al., 2019; Wang et al., 2014; Weeks, 1963). In addition, Figs. 2e and 2f indicate large differences in the shapes of melting peaks. The first observation is related to the width of the melting peaks. Full width at half maximum (FWHM) for slowly cooled (SCs) samples is between 5-6 K (5 K for PP-A and 6 K for PP-H), while in the case of quenched (Qs) samples, it is almost twice as large, between 9-11 K (9 K for PP-A and 11 K for PP-H). Combining DSC with WAXD data, it can be concluded that the smaller (larger) the crystallites, the broader (narrower) the melting peak, revealing a large distribution of crystal defect concentration and size in the crystalline core of quenched (Qs) samples (Seguela et al., 1999). The second observation is connected with the temperatures at which endotherms start to separate from the baseline (green arrows (1) in Figs. 2e and 2f). These onset temperatures are shifted for 20-25 K towards lower temperatures in the case of slowly cooled (SCs) samples compared to quenched (Qs) ones, but even in this case, they are located above 375 K. As we know, this phenomenon has not been discussed in the literature so far, and its interpretation is not simple. Probably, in the case of slowly cooled (SCs) samples, an increase in crystallite size and degree of crystallinity as a consequence has a larger presence of low-temperature component in the melting endotherm, probably due to the large diversity in RAF segment (in concentration and size) containing strained molecules. Enthalpy determined between points 1 and 2 on the thermograms also indicates a significantly larger presence of these rigid-amorphous (RAF) segments in the case of slowly cooled (SCs) samples compared to quenched (Qs) one. Since this fraction start to play role at temperatures higher than 100 °C, it can be, at least partially, connected with increased chain mobility in interphase, i.e., softening of RAF, and due to reduction of stress at the points of entry of tie chains into the lamellae as a result have partial release of accumulated energy. From all of the above, it can be concluded that very slow cooling after melting, in the case of commercial PP, results in a monoclinic α phase with large spherulites, high content of the crystalline phase, large well-ordered crystallites with more uniform size distribution, but also with a significant presence of of low-temperature component in the melting endotherm probably due to large diversity in RAF segment (in concentration and size) containing molecules restricted by well-developed crystallites organized in crystalline superstructures i.e., spherulites. Thus, fiber-like formations with more or less restricted mobility, previously observed at the spherulite boundaries of slowly cooled (SCs) samples, and which cannot be inserted into spherulites and are mostly composed of tie chains, chain loops, etc., can be connected with RAF containing a bundle of strained molecules. At elevated temperatures, increased molecular mobility in the RAF phase will result in reduction of stress at the points of entry of tie chains into the lamellae and consequently at least partial reduction of stress at the points of entry of fiber-like formations into spherulites; however, this will take place at much lower temperatures than ones required for the melting of crystalline phase.

3.5. DRS Study

Dielectric relaxation spectroscopy (DRS), also known as dynamic dielectric spectroscopy (DDS), is a powerful tool to study the structure and molecular mobility of dipolar polymers (Arranz-Andrés

 doi:10.20944/preprints202505.0754.v1

et al., 2007; Banford et al., 1996b; Brandrup, 1975; Castejón, 2001; Dintilhac et al., 2023; Fouracre et al., 1999; Gitsas and Floudas, 2008; Hara, 1967; Hoyos et al., 2007; Jourdan et al., 1989; McCrum, 1964; Olivares et al., 1999; Perepechko, 1977; Pluta and Kryszewski, 1987; Quijada-Garrido et al., 1997; Read, 1990; Sakai et al., 2005; Starkweather et al., 1992; Suljovrujic, 2005, 2009a; Suljovrujic et al., 2010; Tiemblo et al., 2002; Umemura, 1982). PP, as well as PE (another thermoplastic member of the polyolefin (PO) family), are basically nonpolar (Suljovrujic, 2002, 2012; Wang et al., 2024), however, measurable dielectric (loss) signal owes to the fact that it is always slightly oxidized, thus containing polar groups such as carbonyl, peroxy, or hydroperoxy which can be considered as tracer groups reflecting the motion of the polymer chains (Dintilhac et al., 2023; Hedvig, 1977; Suljovrujic, 2005; Suljovrujic et al., 1999); presence of impurities (residual catalysts, antioxidants, etc.) also increase dielectric response (Hedvig, 1977). Due to the low polarity, good mechanical properties, and heat resistance, PP has been widely used as electrical insulation, e.g., for cables and as a dielectric in power capacitors (Fournie, 1990; Jia et al., 2022; Li et al., 2024; Montanari, 2004; Zhuravlev, 2002); this is another reason for growing interest in the investigation of dielectric phenomena of PP-based material (Zhang et al., 2022; Zhang et al., 2024). DRS, together with thermally stimulated discharge current (TSDC) measurements, can also be used to test the oxidative degradation and deterioration of PO cable insulation (Kostoski et al., 2004; Suljovrujic, 2001; Suljovrujic et al., 2013; Suljovrujic et al., 2010). Taking into account certain specificities, the investigation of the motion of the polymer chains and thermodynamic transitions by DRS, generally, corresponds to dynamic mechanical analysis (DMA) findings, which is most often used in the case of PP (Beuguel et al., 2018; Bohning, 2005; Quijada-Garrido et al., 1997).

In relaxation studies, PP displays four mechanical/dielectric relaxations, designated as α, β, γ and δ in the order of decreasing temperature, in addition to the melting point (Arranz-Andrés et al., 2007; Banford et al., 1996a; Brandrup, 1975; Castejón, 2001; Fouracre et al., 1999; Gitsas and Floudas, 2008; Hara, 1967; Hoyos et al., 2007; Jourdan et al., 1989; McCrum, 1964; Olivares et al., 1999; Perepechko, 1977; Pluta and Kryszewski, 1987; Quijada-Garrido et al., 1997; Read, 1990; Sakai et al., 2005; Starkweather et al., 1992; Suljovrujic, 2009a; Suljovrujic et al., 2010; Tiemblo et al., 2002; Umemura, 1982). The origins of these relaxations have been studied in the past, mainly by mechanical measurements. However, a few dielectric studies are also available (Arranz-Andrés et al., 2007; Banford et al., 1996b; Castejón, 2001; Fouracre et al., 1999; Gitsas and Floudas, 2008; Hara, 1967; Hoyos et al., 2007; Jourdan et al., 1989; McCrum, 1964; Olivares et al., 1999; Perepechko, 1977; Pluta and Kryszewski, 1987; Quijada-Garrido et al., 1997; Read, 1990; Sakai et al., 2005; Starkweather et al., 1992). Although some detailed molecular assignments are still open to debate, the fundamentals of the basic relaxation processes are apparent. The α and β relaxations are undoubtedly connected with the crystalline and amorphous phases, respectively. According to Jourdan et al. (Jourdan et al., 1989), the α relaxation is primarily associated with a relaxation of defects in the crystalline phase, with the rigid-amorphous fraction (RAF) also contributing to this process. This relaxation has a multiple nature, consisting of two or even more processes in the α relaxation zone (Pluta and Kryszewski, 1987; Suljovrujic et al., 2010; Tiemblo et al., 2002). The β relaxation is attributed to the glass transition in the amorphous phase of iPP. According to different authors, the γ relaxation is due to the localized (most probably crank-shaft type) motions of either chain ends or branches associated with the amorphous phase (Olivares et al., 1999; Pluta and Kryszewski, 1987; Quijada-Garrido et al., 1997), although initially it was also proposed to arise from the crystalline phase. In dielectric relaxation measurements, iPP may also exhibit a fourth relaxation, mainly below 100 K, which is named the δ process; this relaxation is weak or absent and is attributed to the hindered rotation of CH_3 groups (Brandrup, 1975; Starkweather et al., 1992).

In the case of PP, as we know, DRS has not been used to investigate the structure and relaxation of slowly cooled (SCs) samples, while we used it to investigate structure and relaxation in differently modified quenched (Qs) samples (Milicevic et al., 2014; Suljovrujic, 2009a, 2012). Namely, due to the wide application of PP in medical devices and the necessity for ionizing radiation sterilization of such products, DRS was previously used successfully not only for investigation of structural relaxation in

 doi:10.20944/preprints202505.0754.v1

mesomorphic (smectic) phase but also to obtain valuable information about the level of overall oxidation and distribution of oxidation species within regions with different ordering (Suljovrujic et al., 2024; Suljovrujic et al., 2010). Herein, to investigate the influences of different processing conditions, dielectric loss spectra for (Qs) and slowly cooled (SCs) samples are presented in Figs. 2g and 2h, respectively. The presence of three relaxations can be clearly confirmed - the high-temperature α relaxation (located around 350 K for Qs and at 370 K for SCs samples), β relaxation (around 300 K), and low-temperature γ relaxation (around 250 K). The presence of the fourth δ relaxation, which occurs at temperatures below 150 K, can also be confirmed. Still, this relaxation is barely noticeable, especially in the case of SCs spectra, and will not be discussed further.

Before starting the discussion, it should be kept in mind that SCs samples during slow cooling from the melt have more prolonged exposure to high temperatures and consequently can have a slightly larger amount of oxygen-containing groups in the structure due to thermal degradation (Qian et al., 2011). On the other hand, dielectric loss spectra are sensitive even to a minimal increase of polar groups in the molecular structure of apolar polymers such as PP (Suljovrujic et al., 2021). However, by comparing Qs and SCs dielectric loss spectra, in the case of γ relaxation, only a difference in intensity can be noticed, and it is much larger in the case of Qs samples compared to SCs ones; otherwise, shape, position, and determined activation energy (35-40 kJ/mol) are only slightly affected. Since this relaxation originates from the amorphous phase, it is expected that with an increase in the degree of crystallinity, which is the case with SCs samples, the intensity of this relaxation decreases. The dynamic mechanical investigation of iPP thermo-oxidative degradation indicated that the initiation of thermal oxidation is concomitant with a partial vanishing of γ relaxation (Hoyos et al., 2007; Olivares et al., 1999; Tiemblo et al., 2002). Furthermore, complete disappearance of dielectric γ relaxation was observed with gamma irradiation in the air (Suljovrujic, 2009a, 2012), as in the case of ultraviolet rays (Hara, 1967; Perepechko, 1977), confirming its intense sensitivity to oxidative degradation.

Nevertheless, further comparison of the dielectric loss spectra for Qs and SCs samples indicates that the location of β relaxation is almost unaffected, while in the case of α relaxation, a significant shift to higher temperature is noticeable in the case of SCs samples (370 K) comparing to Qs ones (350 K). In addition, a significantly broader α peak can be observed in the SCs samples compared to the Qs ones, while the peak shapes of β relaxation are the same. Furthermore, a larger intensity of α relaxation is observed for SCs samples, while the ratio between intensities of α and β relaxation (I_α/I_β) increases from 1.5 (for Qs) to almost 3 (for SCs), favoring α relaxation increase in the case of SCs samples. All of these features can be associated with large differences in the degree of crystallinity and crystallite size between Qs (i.e., mesomorphic (smectic) form previously characterized by low content of crystalline phase with small crystallites) and SCs samples (i.e., developed monoclinic form previously characterized by high content of crystalline phase with large crystallites size and developed spherulites). Thus, the increase in intensity and the shift in location to higher temperature obtained for SCs samples can be explained by a much larger crystalline phase content and significantly larger crystallite size, respectively (Di Sacco et al., 2021). Such behavior of α relaxation can be well related to the behavior of the crystalline phase during melting obtained by DSC measurements. Even a significantly broader α peak in the case of SCs samples can be connected with the increased presence of low-temperature components in the melting endotherm, probably due to the wide dissipated distribution of the RAF segment (in concentration and size), containing strained molecules.

Furthermore, in the case of dielectric loss spectra of the Qs sample presented in Fig. 2g, experimental data are fitted with more or less success by only one α relaxation peak, while the insert in Fig. 2g represents the same experimental data in α region much better fitted with three split peaks confirming multiple nature of α relaxation in mesomorphic (smectic) phase, consisting of two or even more processes in the α relaxation zone. Such α relaxation behavior in the case of mesomorphic (smectic) form is also confirmed by DMA; according to Seguela et al., α_1 relaxation, which occurs around 330 K indicates higher energy absorption due to more intense molecular mobility and can be

 doi:10.20944/preprints202505.0754.v1

connected with cold crystallization, i.e., crystallization from mesophase (Seguela et al., 1999). Activation energies for β and α relaxation are calculated by Vogel-Fulcher-Tammann-Hesse (VFTH) and Arrhenius equations, respectively, using the procedure given in more detail in the literature (Suljovrujic, 2012). Obtained difference in activation energies between Qs and SCs samples is relatively small for both relaxation and, in the case of β relaxation, ranges from 480 to 560 kJ/mol (with dynamic fragility m from 98 to 105), while for α relaxation, is in the interval from 110 to 90 kJ/mol, respectively. Results obtained from dielectric loss spectra also indicate that the restriction in movements and reorganization of chains associated with the crystalline phase are reduced at elevated temperatures. The occurrence of α relaxation is undoubtedly connected with the crystalline phase, and it is due to a relaxation of defects in the crystalline phase. Still, the rigid-amorphous fraction (RAF) also contributes to this process. However, this relaxation occurs at much lower temperatures than the ones required for the melting of the crystalline phase.

3.6. Mechanical Study

Among the physical properties, the mechanical ones are probably the most important for the use of PP in a wide range of applications, from medical and pharmaceutical to packaging and automotive. The mechanical properties of PP, as a plastic or a fiber, are widely investigated because of its sizeable structural complexity, the existence of different stereochemical configurations, polymorphic nature, different processing conditions, exposure to different external conditions, stretching and fiber applications, radiation sterilization of medical devices, recycling, blending with other polymers, application in composites, etc. Nevertheless, several new studies in which the mechanical properties of PP are in focus indicate that this area is still of great interest not only to industry but also to the academic community (Sharaf and Kloczkowski, 2024; Zhang et al., 2024). In the introduction section, we have discussed the mechanical properties of PP and the influence of isotacticity. In general, mechanical properties of PP, such as softening point, rigidity, Young's modulus, strength, and toughness, are improved by increasing the degree of isotacticity as well as by the increase in crystallinity of the same grade iPP due to processing condition (Fukuda et al., 2023; Pasquini, 2005; Yamada et al., 1998). Herein, the focus is on the influence of processing conditions on commercial PP with high isotacticity. Samples obtained by two opposite cooling procedures after compression molding, rapid quenching and slow cooling, which represent border conditions in the case of industrial processing, are subject to investigation of tensile properties and stress-relaxation mechanical behavior in an attempt to gain profound insight into the structure-to-mechanical properties relations.

Typical tensile stress-strain diagrams of quenched (Qs) and slowly cooled (SCs) samples for four different grade commercial PPs are presented in Fig. 3: PP-A (a), PP-H (b), PP-T (c), and PP-H (d). Analyzing the stress-strain curves for the slowly cooled SCs samples was challenging because strips (dumbbell-shaped specimens) were very fragile. The first look at Figs. 3a-d shows that SCs sample stress-strain curves look like those in brittle materials, unlike the curves of Qs samples, which are typical for ductile materials. Namely, the curve of SCs samples does not show the yield point and plastic deformation stage, thus indicating that slowly cooled commercial PPs exhibited brittle behavior in general. While Qs samples undergo elastic as well as plastic deformation and elongate more than 500 % before breakage, SCs samples show only elastic deformation, and in the vicinity of the yield point (i.e., initiation point of plastic deformation), they break with elongations of less than 15% (Fig. 3 i). Total absence of plasticity in SCs samples, evident from the obtained stress-strain curves at room temperature, is more or less expected since most literature data for highly crystalline (slowly cooled and annealed) iPP, with some exceptions (Fukuda et al., 2023; Nitta and Yamaguchi, 2006), confirm brittle behavior with missing or poor plasticity (Arranz-Andrés et al., 2007; Kida et al., 2023; Nitta, 2018). As the temperature at which stress-strain measurements are performed gets larger, plasticity appears (Li et al., 2020). This can be explained by the fact that in highly crystalline iPP, at room and other test temperatures that are close enough to the glass transition temperature (T_g), structural restrictions caused by high crystallinity, large crystallites, and the presence of spherulites

 doi:10.20944/preprints202505.0754.v1

act as it is still in the glassy state. In the case of Qs samples, despite the difference in intermediate form as well as crystallinity and crystallite size (which are much lower than in the case of SCs samples) between PP-A and PP-H samples, very similar stress-strain behavior is observed; at room temperature, Qs samples show intensive plastic deformation. After propagation of a plastic instability (necking) over the whole sample length, strain-hardening occurs as a result of chain unfolding and orientation involving the so-called fibrillar transformation. Two different mechanisms of plastic deformation of crystalline polymers have been proposed in the literature and well discussed by Makarewicz et al. (Makarewicz et al., 2022). The first one is based on the phenomenon of emission of dislocations from the edges of the lamellar crystals and their movement within crystals via crystallographic slips, which was proposed by Peterson (Peterson, 1966, 1968). The second mechanism of yielding of semicrystalline polymers assumes non-crystallographic changes of the initial crystalline skeleton, leading to the formation of completely new crystalline structures dependent mainly on the deformation temperature. Peterlin and co-workers proposed the micro necking model, which changed the crystal lamellae from folded morphology into a partially unfolded fibrillar one (Morosoff and Peterlin, 1972; Peterlin, 1971). According to this model, plastic deformation consists of three stages in the cold drawing of crystalline polymers: the plastic deformation of the original spherulitic structure, the discontinuous transformation of the spherulitic into fiber structure by micronecking, and the plastic deformation of the fiber structure. Because of its commercial importance, much work has been directed toward understanding the cavitation and plastic deformation of semicrystalline polymers as well as fiber structures (Aboulfaraj et al., 1995; Ariyama et al., 1997; Butler et al., 1995; Chen et al., 2015; Chodák, 1998; Furuta and Kojima, 1986; G'sell et al., 1997; Kim et al., 2021; Liparoti et al., 2021; Liu et al., 1986; Milicevic et al., 2012; Milicevic et al., 2007b; Na and Lv, 2007; Pawlak et al., 2013; Séguéla, 2002; Shirinbayan et al., 2024; Suljovrujic, 2009b). Stress-strain measurements were also used to investigate the transformation of the mesomorphic (smectic) phase into the monoclinic (α) phase by annealing and the difference between these phases (Arranz-Andrés et al., 2007; Fukuda et al., 2023; Kida et al., 2023; Nitta and Yamaguchi, 2006; Seguela et al., 1999). According to some of them (Fukuda et al., 2023; Kida et al., 2023; Nitta and Yamaguchi, 2006; Seguela et al., 1999), despite the presence of monoclinic (α) phase with spherulites, annealed iPP specimens after quenching possess plastic deformation. This is probably due to an overall lower degree of crystallinity, thinner crystallite lamellae, and much smaller spherulites than in the case of slowly cooled samples from a melt.

 doi:10.20944/preprints202505.0754.v1

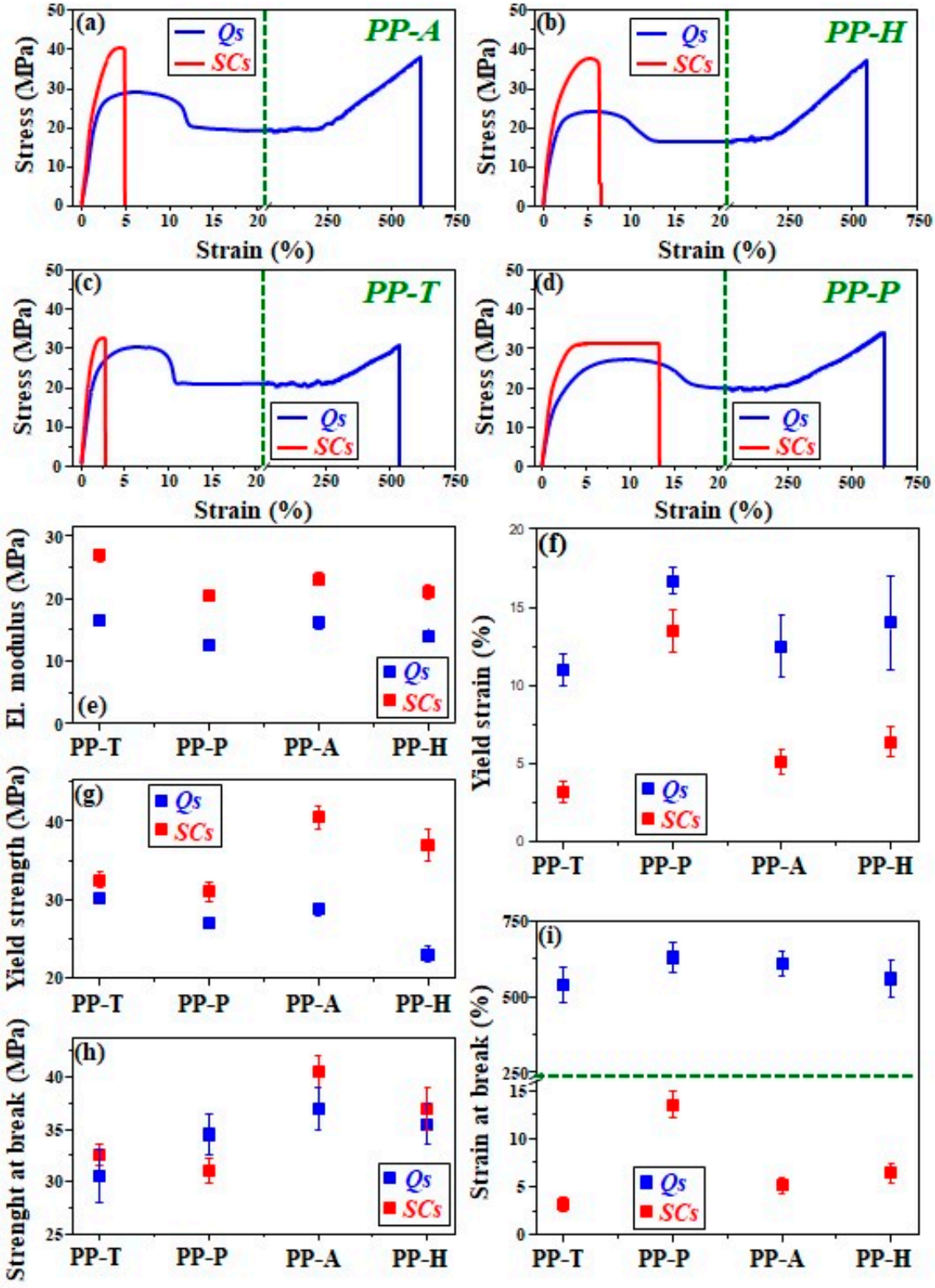

Figure 3. A typical tensile stress-strain diagrams of quenched (*Qs*) and slowly cooled (*SCs*) samples for four different PPs: (a) PP-A, (b) PP-H, (c) PP-T, and (d) PP-H; Variation for *Qs* and slowly cooled (*SCs*) samples in Elastic Modulus (e), Yield strain (f), Yield strength (g), Strength at break (h), and Strain at break, i.e., Total Elongation (i) with PP type.

 doi:10.20944/preprints202505.0754.v1

Mechanical parameters are presented in Figs. 3 e-i to better understand how processing conditions influence the structure-to-mechanical properties relations for commercial PPs. Thus, elastic (Young) modulus, yield strain, yield strength, strength at break, and strain at break (elongation), determined from stress-strain curves, are presented as a function of PP type for quenched (Qs) and slowly cooled (SCs) samples. As can be seen from Figs. 3e and 3g, Young's modulus and yield strength are higher in SCs samples due to larger crystallinity and more developed crystal architecture than in the case of Qs samples. In the case of Qs samples, strength at break, due to the formation of a well-developed fibrillar structure with polymeric chains preferentially oriented along the stretching direction (Milicevic et al., 2012), increases and may exceed the yield strength of the corresponding SCs sample; that is evident for PP-P, i.e., PP with ionizing radiation stabilizers. In general, the presence of a nucleating agent can change the spherulite size of PP, increase the crystallization rate, and decrease the spherulite size (An et al., 2019). However, commercial polypropylenes with specific additives (PP-T and PP-P) show similar behavior and fit pretty well with others within this study.

4. Conclusions

Due to their complex and hierarchical structure and variety in industrial processing techniques, semicrystalline polymers such as PP require more detailed, systematic studies, especially those employing modern approaches and experimental techniques. In this work, two opposite cooling procedures after compression molding, rapid quenching and slow cooling, which represent boundary cases in industrial processing, were applied. The resulting differences in microstructure, crystallinity, and properties were significant, regardless of the starting material being the same commercial PP with a high isotactic fraction. The numerous investigations only partially cover different segments of this topic, suggesting a need for inclusive studies that go beyond fragmented investigations in existing literature. Our results are broadly consistent with the comprehensive literature data, which are contradictory in some segments, reflecting the inherent complexity of the system.

While the slow cooling after melting of different grade commercial PPs results in a monoclinic (α) form with a well-developed spherulite texture, high degree of crystallinity, and large crystallites, quenching in an ice-water mixture after melting fails in an attempt to produce such ordered structures. Depending on PP grade, quenching yields a clear mesomorphic (smectic) form or a more ordered but still intermediate form comprising both monoclinic (α) and mesomorphic (smectic) phase. Surface microstructures studied by optical microscopy (OM) and scanning electron microscopy (SEM) in the case of SCs samples show great spherulites with large cavities and fiber-like formations at the spherulite boundaries, in contrast to the relatively smooth, non-porous Qs samples' surfaces with no signs of significant crystalline architecture. Wide angle X-ray diffraction (WAXD) was used to determine parameters of crystalline architecture, revealing in the case of SCs significantly higher degree of crystallinity ($\chi \geq 55$ %) and crystallite size ($L_{(110)}$=17.5 nm and $L_{(110)}$=21.1 nm, depending on the PP type) in comparison to Qs samples (for mesomorphic (smectic) form χ<30 % with $L_{(110)} \leq 3$ nm, while for more ordered but still intermediate form χ=36% with $L_{(110)}$=9.5 nm). Thus, the results obtained for the degree of crystallinity are in good agreement with FTIR and DSC findings. The higher melting temperature in the case of SCs samples is attributed to lamellar thickening, promoted by slow cooling after melting, leading to a large increase in crystallite dimension and the formation of very thick lamella with higher thermal stability and perfection. The presence of a low-temperature component in the melting endotherm of SCs samples is connected with a large diversity in RAF segments (in concentration and size) containing strained molecules. DRS was used, possibly for the first time, to study the difference in molecular mobility between the iPP mesomorphic (smectic) and α-monoclinic phase. The two most important relaxations were investigated: β (glass transition) relaxation associated with the amorphous phase and α relaxation connected with the crystalline phase, which is due to a relaxation of defects in the crystalline phase, with a contribution of the rigid-amorphous fraction (RAF) to this process. Differences in dielectric loss spectra were

 doi:10.20944/preprints202505.0754.v1

successfully connected with a significant discrepance in the degree of crystallinity and crystallite size between Qs and SCs samples. Thus, the increase in α relaxation intensity and the shift in location to higher temperature obtained for SCs samples are explained by a much larger crystalline phase content and significantly larger crystallite size, respectively. DRS data in the α relaxation region also confirmed that the restriction in movements and reorganization of chains associated with the crystalline phase are reduced at elevated temperatures.

Our results show that mechanical properties, probably the most important for wide PP industrial applications, are strongly influenced by different preparation methods, such as rapid quenching and slow cooling after melting. At room temperature, rapid quenched (Qs) samples show stress-strain curves typical for ductile materials and undergo elastic as well as plastic deformation with elongation larger than 500 % before breakage. On the other hand, slowly cooled (SCs) samples show typical behavior for brittle materials, i.e., with elastic deformation and a break in the yield region with elongations of less than 15%. This can be explained by the fact that in SCs samples, at room and other test temperatures that are close enough to the glass transition temperature (T_g), structural restrictions caused by high crystallinity, large crystallites, and the presence of spherulites act as it is still in the glassy state. Young's modulus and yield strength are significantly higher in SCs samples due to larger crystallinity and more developed crystal architecture. In the case of Qs samples, strength at break increases and can become larger than the corresponding SCs sample yield strength, due to forming a well-developed fibrillar structure with polymeric chains preferentially oriented along the stretching direction. The stress-strain behavior of PPs with specific additives (one with nucleating and antistatic agents and the other with ionizing radiation stabilizers) is in good agreement with other investigated PPs.

The comprehensive multi-technique approach that combines microstructural analysis, crystallographic studies, and spectroscopy with calorimetric, DRS, and mechanical studies provides a holistic view of polypropylene's behavior under different processing conditions. The presented findings can be applied to optimize polypropylene processing conditions for specific applications where crystallinity, thermal, and mechanical properties play a crucial role, such as in packaging, automotive, and biomedical applications.

Author Contributions: ConceptualizationE.S. and S.G.; methodology, E.S.,D.M..; formal analysis, E.S, D.M., K.Dj.,Z.R.M., G.S.,S.G; investigation, E.S, D.M., K.Dj.,Z.R.M., G.S.,S.G; resources, E.S; writing—original draft preparation,E.S; writing—review and editing, E.S., D.M., K.Dj.,S.G; visualization, E.S.,K.Dj.; All authors have read and agreed to the published version of the manuscript.

Funding: Please add: "This research received no external funding" or "This research was funded by NAME OF FUNDER, grant number XXX" and "The APC was funded by XXX". Check carefully that the details given are accurate and use the standard spelling of funding agency names at https://search.crossref.org/funding. Any errors may affect your future funding.

Data Availability Statement: This study did not generate any datasets.

Acknowledgments: This work was financially supported by the Ministry of Science, Technological Development, and Innovation of the Republic of Serbia (Contract No. 451–03–136/2025–03/200017) and the IAEA. The research was performed as an integral part of a Research Project titled "Comparative study of e-beam and gamma radiation effects in polyolefins commonly used in medical devices" (IAEA Research Contract No: 24728), which forms a part of the IAEA Coordinated Research Project F23035, entitled "Radiation Effect on Polymer Materials Commonly Used in Medical Devices".

Conflicts of Interest: The authors declare no conflicts of interest.

References

Aboulfaraj, M., G'Sell, C., Ulrich, B., Dahoun, A., 1995. In situ observation of the plastic deformation of polypropylene spherulites under uniaxial tension and simple shear in the scanning electron microscope. Polymer 36, 731-742. https://doi.org/10.1016/0032-3861(95)93102-R

 doi:10.20944/preprints202505.0754.v1

Addeo, A., 2005. Polypropylene Handbook. Hanser Gardner

Amer, I., van Reenen, A., Mokrani, T., 2015. Molecular weight and tacticity effect on morphological and mechanical properties of Ziegler–Natta catalyzed isotactic polypropylenes. Polímeros 25, 556-563. http://dx.doi.org/10.1590/0104-1428.2158

An, H., Li, X., Geng, Y., Wang, Y., Wang, X., Li, L., Li, Z., Yang, C., 2008. Shear-Induced Conformational Ordering, Relaxation, and Crystallization of Isotactic Polypropylene. The Journal of Physical Chemistry B 112, 12256-12262. https://doi.org/10.1021/jp802511b

An, Y., Wang, S., Li, R., Shi, D., Gao, Y., Song, L., 2019. Effect of different nucleating agent on crystallization kinetics and morphology of polypropylene. e-Polymers 19, 32-39. https://doi.org/doi:10.1515/epoly-2019-0005

Androsch, R., 2008. In Situ Atomic Force Microscopy of the Mesomorphic−Monoclinic Phase Transition in Isotactic Polypropylene. Macromolecules 41, 533-535. https://doi.org/10.1021/ma702334q

Androsch, R., Di Lorenzo, M.L., Schick, C., Wunderlich, B., 2010. Mesophases in polyethylene, polypropylene, and poly(1-butene). Polymer 51, 4639-4662. https://doi.org/10.1016/j.polymer.2010.07.033

Ariff, Z., Ariffin, A., Jikan, S., Abdul Rahim, N., 2012. Rheological Behaviour of Polypropylene Through Extrusion and Capillary Rheometry, in: Dogan, F. (Ed.), Polypropylene pp. 29-48.

Ariyama, T., Mori, Y., Kaneko, K., 1997. Tensile properties and stress relaxation of polypropylene at elevated temperatures. Polym. Eng. Sci. 37, 81-90. https://doi.org/10.1002/pen.11647

Arranz-Andrés, J., Peña, B., Benavente, R., Pérez, E., Cerrada, M.L., 2007. Influence of isotacticity and molecular weight on the properties of metallocenic isotactic polypropylene. Eur. Polym. J. 43, 2357-2370. https://doi.org/10.1016/j.eurpolymj.2007.03.034

Arvidson, S.A., Khan, S.A., Gorga, R.E., 2010. Mesomorphic−α-Monoclinic Phase Transition in Isotactic Polypropylene: A Study of Processing Effects on Structure and Mechanical Properties. Macromolecules 43, 2916-2924. https://10.1021/ma1001645

Auriemma, F., De Rosa, C., Corradini, P., 2005. Solid Mesophases in Semicrystalline Polymers: Structural Analysis by DiffractionTechniques, in: Allegra, G. (Ed.), Interphases and Mesophases in Polymer Crystallization II. Springer Berlin Heidelberg, Berlin, Heidelberg, pp. 1-74.

Banford, H.M., Fouracre, R., Faucitano, A., Buttafava, A., Martinotti, F., 1996a. The influence of -irradiation and chemical structure on the dielectric properties of PP. Radiat. Phys. Chem. 48, 129-130. https://doi.org/10.1016/0969-806X(96)00025-4

Banford, H.M., Fouracre, R.A., Faucitano, A., Buttafava, A., Martinotti, F., 1996b. The influence of chemical structure on the dielectric behavior of polypropylene IEEE Transactions on Dielectrics and Electrical Insulation 3, 594-598. https://doi.org/10.1109/94.536740

Bassett, D.C., 1981. Principles of polymer morphology. Cambridge [Eng.], New York.

Bassett, D.C., Keller, A., Mitsuhashi, S., 1963. New features in polymer crystal growth from concentrated solutions. Journal of Polymer Science Part A: General Papers 1, 763-788. https://doi.org/10.1002/pol.1963.100010215

Bassett, D.C., Olley, R.H., 1984. On the lamellar morphology of isotactic polypropylene spherulites. Polymer 25, 935-943. https://doi.org/10.1016/0032-3861(84)90076-4

Bassett, D.C., Vaughan, A.S., 1985. On the lamellar morphology of melt-crystallized isotactic polystyrene. Polymer 26, 717-725. https://doi.org/10.1016/0032-3861(85)90109-0

Beuguel, Q., Mija, A., Vergnes, B., Peuvrel-Disdier, E., 2018. Structural, thermal, rheological and mechanical properties of polypropylene/graphene nanoplatelets composites: Effect of particle size and melt mixing conditions. Polym. Eng. Sci. 58, 1937-1944. https://doi.org/10.1002/pen.24803

Bogoeva-Gaceva, G., 2014. Advances in polypropylene based materials. Contributions, Section of Natural, Mathematical and Biotechnical Sciences 35, 121-138. https://10.20903/csnmbs.masa.2014.35.2.58

Bohning, M., Goering, H., Fritz, A., Brzezinka, K.-W., Turky, G., Schönhals, A., Schartel, B., 2005. Dielectric study of molecular mobility in poly(propylene-graft-maleic anhydride)/clay nanocomposites. Macromolecules 38, 2764-2774. https://doi.org/10.1021/ma048315c

Brandrup, J., Immergut, E.H., Grulke, E.A., 1999. Polymer Handbook Wiley-Interscience, New York.

Brandrup, J., Immergut EH., 1975. Polymer Handbook. Wiley, New York.

 doi:10.20944/preprints202505.0754.v1

Brucato, V., Piccarolo, S., La Carrubba, V., 2002. An experimental methodology to study polymer crystallization under processing conditions. The influence of high cooling rates. Chem. Eng. Sci. 57, 4129-4143. https://doi.org/10.1016/S0009-2509(02)00360-3

Brückner, S., Meille, S.V., Petraccone, V., Pirozzi, B., 1991. Polymorphism in isotactic polypropylene. Prog. Polym. Sci. 16, 361-404. https://doi.org/10.1016/0079-6700(91)90023-E

Burfield, D.R., Loi, P.S.T., 1988. The use of infrared spectroscopy for determination of polypropylene stereoregularity. J. Appl. Polym. Sci. 36, 279-293. https://doi.org/10.1002/app.1988.070360203

Butler, M.F., Donald, A.M., Bras, W., Mant, G.R., Derbyshire, G.E., Ryan, A.J., 1995. A Real-Time Simultaneous Small- and Wide-Angle X-ray Scattering Study of In-Situ Deformation of Isotropic Polyethylene. Macromolecules 28, 6383-6393. https://doi.org/10.1021/ma00123a001

Caldas, V., Brown, G.R., Nohr, R.S., MacDonald, J.G., Raboin, L.E., 1994. The structure of the mesomorphic phase of quenched isotactic polypropylene. Polymer 35, 899-907. https://doi.org/10.1016/0032-3861(94)90931-8

Castejón, M.L., Tiemblo P, Gómez-Elvira JM., 2001. Photo-oxidation of thick isotactic polypropylene films. II. Evolution of the low temperature relaxations and of the melting endotherm along the kinetic stages. Polym. Degrad. Stab. 71, 99-111. https://doi.org/10.1016/S0141-3910(00)00159-2

Chan, C.-M., Li, L., 2005. Direct Observation of the Growth of Lamellae and Spherulites by AFM, in: Kausch, H.-H. (Ed.), Intrinsic Molecular Mobility and Toughness of Polymers II. Springer Berlin Heidelberg, Berlin, Heidelberg, pp. 1-41.

Chang, B., Schneider, K., Vogel, R., Heinrich, G., 2017. Influence of Annealing on Mechanical αc-Relaxation of Isotactic Polypropylene: A Study from the Intermediate Phase Perspective. Macromol. Mater. Eng. 302, 1700291. https://doi.org/10.1002/mame.201700291

Chen, W., Li, X.-y., Liu, Y.-p., Li, J., Zhou, W.-m., Chen, L., Li, L.-b., 2015. The spatial correlation between crystalline and amorphous orientations of isotactic polypropylene during plastic deformation: An in situ observation with FTIR imaging. Chin. J. Polym. Sci. 33, 613-620. https://doi.org/10.1007/s10118-015-1613-3

Chen, W., Zhang, Q., Zhao, J., Li, L., 2020. Molecular and thermodynamics descriptions of flow-induced crystallization in semi-crystalline polymers. Journal of Applied Physics 127. https://doi.org/10.1063/5.0012376

Cheng, S.Z.D., Janimak, J.J., Zhang, A., Hsieh, E.T., 1991. Isotacticity effect on crystallization and melting in polypropylene fractions: 1. Crystalline structures and thermodynamic property changes. Polymer 32, 648-655. https://doi.org/10.1016/0032-3861(91)90477-Z

Chodák, I., 1998. High modulus polyethylene fibres: preparation, properties and modification by crosslinking. Prog. Polym. Sci. 23, 1409-1442. https://doi.org/10.1016/S0079-6700(98)00006-9

Cohen, Y., Saraf, R., 2001. A direct correlation function for mesomorphic polymers and its application to the 'smectic' phase of isotactic polpropylene. Polymer 42, 5865-5870. https://doi.org/10.1016/S0032-3861(00)00914-9

Cong, Y., Hong, Z., Qi, Z., Zhou, W., Li, H., Liu, H., Chen, W., Wang, X., Li, L., 2010. Conformational Ordering in Growing Spherulites of Isotactic Polypropylene. Macromolecules 43, 9859-9864. https://doi.org/10.1021/ma1019686

Cong, Y., Hong, Z., Zhou, W., Chen, W., Su, F., Li, H., Li, X., Yang, K., Yu, X., Qi, Z., Li, L., 2012. Conformational Ordering on the Growth Front of Isotactic Polypropylene Spherulite. Macromolecules 45, 8674-8680. https://doi.org/10.1021/ma301595k

De Rosa, C., Auriemma, F., Circelli, T., Waymouth, R.M., 2002. Crystallization of the α and γ Forms of Isotactic Polypropylene as a Tool To Test the Degree of Segregation of Defects in the Polymer Chains. Macromolecules 35, 3622-3629. https://doi.org/10.1021/ma0116248

De Rosa, C., Auriemma, F., Tarallo, O., Malafronte, A., Di Girolamo, R., Esposito, S., Piemontesi, F., Liguori, D., Morini, G., 2017. The "Nodular" α Form of Isotactic Polypropylene: Stiff and Strong Polypropylene with High Deformability. Macromolecules 50, 5434-5446. https://doi.org/10.1021/acs.macromol.7b00787

Di Lorenzo, M.L., Righetti, M.C., 2018. Crystallization-induced formation of rigid amorphous fraction. POLYMER CRYSTALLIZATION 1, e10023. https://doi.org/10.1002/pcr2.10023

 doi:10.20944/preprints202505.0754.v1

Di Sacco, F., Saidi, S., Hermida-Merino, D., Portale, G., 2021. Revisiting the Mechanism of the Meso-to-α Transition of Isotactic Polypropylene and Ethylene–Propylene Random Copolymers. Macromolecules 54, 9681-9691. https://doi.org/10.1021/acs.macromol.1c01904

Dintilhac, N., Lewandowski, S., Planes, M., Lectez, A.S., Dantras, E., 2023. Tuning dielectric response of polyethylene by low gamma dose: Molecular mobility study improvement by dipolar probes implementation. J. Non•Cryst. Solids 621, 122606. https://doi.org/10.1016/j.jnoncrysol.2023.122606

Dudic, D., Kostoski, D., Djokovic, V., Dramicanin, M., 2002. Formation and behaviour of low-temperature melting peak of quenched and annealed isotactic polypropylene. Polym. Int. 51, 111-116. https://doi.org/10.1002/pi.803

Dudić, D., Kostoski D, Djoković V, Dramićanin MD., 2002. Formation and behaviour of low-temperature melting peak of quenched and annealed isotactic polypropylene. Polym. Int. 51, 111-116. https://doi.org/10.1002/pi.803

Dudić, D.k., Kostoski, D.a., Djoković, V., Dramićanin, M.D., 2002. Formation and behaviour of low-temperature melting peak of quenched and annealed isotactic polypropylene. Polym. Int. 51, 111-116. https://doi.org/10.1002/pi.803

Farrow, G., 1963. Crystallinity, 'crystallite size' and melting point of polypropylene. Polymer 4, 191-197. https://doi.org/10.1016/0032-3861(63)90025-9

Ferrero, A., Ferracini, E., Mazzavillani, A., Malta, V., 2000. A New X-Ray Study of the Quenched Isotactic Polypropylene Transition by Annealing. Journal of Macromolecular Science, Part B 39, 109-129. https://doi.org/10.1081/MB-100100375

Fouracre, R.A., MacGregor, S.J., Judd, M., Banford, H.M., 1999. Condition monitoring of irradiated polymeric cables. Radiat. Phys. Chem. 54, 209-211. https://doi.org/10.1016/S0969-806X(98)00246-1

Fournie, R., 1990. All film power capacitors. Endurance tests and degradation mechanisms. Bulletin de la Direction des etudes et recherches. Serie B, Reseaux electriques, materiels electriques 1, 1-31.

Fu, X., Jia, W., Li, X., Wang, Y., Wang, Z., Liu, C., Shen, C., Shao, C., 2019. Phase transitions of the rapid-compression-induced mesomorphic isotactic polypropylene under high-pressure annealing. J. Polym. Sci., Part B: Polym. Phys. 57, 651-661. https://doi.org/10.1002/polb.24820

Fukuda, Y., Kida, T., Yamaguchi, M., 2023. Mechanical properties of isotactic polypropylene with nodular or spherulite morphologies. Polym. Eng. Sci. 63, 4043-4050. https://doi.org/10.1002/pen.26504

Furuta, M., Kojima, K., 1986. Morphological study of deformation process for linear polyethylene. Journal of Macromolecular Science, Part B 25, 349-364. https://doi.org/10.1080/00222348608248044

G'sell, C., Favier, V., Hiver, J.M., Dahoun, A., Philippe, M.J., Canova, G.R., 1997. Microstructure transformation and stress-strain behavior of isotactic polypropylene under large plastic deformation. Polym. Eng. Sci. 37, 1702-1711. https://doi.org/10.1002/pen.11818

Geng, Y., Wang, G., Cong, Y., Bai, L., Li, L., Yang, C., 2009. Shear-Induced Nucleation and Growth of Long Helices in Supercooled Isotactic Polypropylene. Macromolecules 42, 4751-4757. https://doi.org/10.1021/ma9004567

Gitsas, A., Floudas, G., 2008. Pressure Dependence of the Glass Transition in Atactic and Isotactic Polypropylene. Macromolecules 41, 9423-9429. https://doi.org/10.1021/ma8014992

Gomez, M.A., Tanaka, H., Tonelli, A.E., 1987. High-resolution solid-state 13C nuclear magnetic resonance study of isotactic polypropylene polymorphs. Polymer 28, 2227-2232. https://doi.org/10.1016/0032-3861(87)90378-8

Guleria, D., Ge, S., Cardon, L., Vervoort, S., den Doelder, J., 2024. Impact of resin density and short-chain branching distribution on structural evolution and enhancement of tensile modulus of MDO-PE films. Polym. Test. 139, 108560. https://doi.org/10.1016/j.polymertesting.2024.108560

Haftka, S., Könnecke, K., 1991. Physical properties of syndiotactic polypropylene. Journal of Macromolecular Science, Part B 30, 319-334. https://doi.org/10.1080/00222349108219480

Haggenmueller, R., Guthy, C., Lukes, J.R., Fischer, J.E., Winey, K.I., 2007. Single Wall Carbon Nanotube/Polyethylene Nanocomposites: Thermal and Electrical Conductivity. Macromolecules 40, 2417-2421. https://doi.org/10.1021/ma0615046

 doi:10.20944/preprints202505.0754.v1

Hanna, L.A., Hendra, P.J., Maddams, W., Willis, H.A., Zichy, V., Cudby, M.E.A., 1988. Vibrational spectroscopic study of structural changes in isotactic polypropylene below the melting point. Polymer 29, 1843-1847. https://doi.org/10.1016/0032-3861(88)90401-6

Hara, T., 1967. Dielectric Property of Some Polymers in Low Temperature Region. Jpn. J. Appl. Phys. 6, 147-150. https://doi.org/10.1143/JJAP.6.147

Hedvig, P., 1977. Dielectric Spectroscopy of Polymers. Academia Kiado, Budapest.

Heinen, W., 1959. Infrared determination of the crystallinity of polypropylene. J. Polym. Sci. 38, 545-547. https://doi.org/10.1002/pol.1959.1203813426

Hendra, P.J., Vile, J., Willis, H.A., Zichy, V., Cudby, M.E.A., 1984. The effect of cooling rate upon the morphology of quenched melts of isotactic polypropylenes. Polymer 25, 785-790. https://doi.org/10.1016/0032-3861(84)90007-7

Hine, P., Broome, V., Ward, I., 2005. The incorporation of carbon nanofibres to enhance the properties of self reinforced, single polymer composites. Polymer 46, 10936-10944. https://doi.org/10.1016/j.polymer.2005.08.076

Hoyos, M., Tiemblo, P., Gómez-Elvira, J.M., 2007. The role of microstructure, molar mass and morphology on local relaxations in isotactic polypropylene. The α relaxation. Polymer 48, 183-194. https://doi.org/10.1016/j.polymer.2006.11.034

Huang, S., Li, H., Jiang, S., 2019. Crystal structure and unique lamellar thickening for poly(l-lactide) induced by high pressure. Polymer 175, 81-86. https://doi.org/10.1016/j.polymer.2019.05.020

Huy, T.A., Adhikari, R., Lüpke, T., Henning, S., Michler, G.H., 2004. Molecular deformation mechanisms of isotactic polypropylene in α- and β-crystal forms by FTIR spectroscopy. J. Polym. Sci., Part B: Polym. Phys. 42, 4478-4488. https://doi.org/10.1002/polb.20117

Imai, M., Kaji, K., 2006. Polymer crystallization from the metastable melt: The formation mechanism of spherulites. Polymer 47, 5544-5554. https://doi.org/10.1016/j.polymer.2005.07.109

Jia, C., Das, P., Kim, I., Yoon, Y.-J., Tay, C.Y., Lee, J.-M., 2022. Applications, treatments, and reuse of plastics from electrical and electronic equipment. Journal of Industrial and Engineering Chemistry 110, 84-99. https://doi.org/10.1016/j.jiec.2022.03.026

Jiang, C., Miao, C., Zhou, J., Yuan, M., 2025. Insights into damage mechanisms and advances in numerical simulation of spherulitic polymers. Polymer 318, 128001. https://doi.org/10.1016/j.polymer.2024.128001

Jiang, Q., Zhao, Y., Zhang, C., Yang, J., Xu, Y., Wang, D., 2016. In-situ investigation on the structural evolution of mesomorphic isotactic polypropylene in a continuous heating process. Polymer 105, 133-143. https://doi.org/10.1016/j.polymer.2016.10.004

Jourdan, C., Cavaille, J.Y., Perez, J., 1989. Mechanical relaxations in polypropylene: A new experimental and theoretical approach. J. Polym. Sci., Part B: Polym. Phys. 27, 2361-2384. https://doi.org/10.1002/polb.1989.090271115

Karger-Kocsis, J., Bárány, T., 2019. Polypropylene Handbook Morphology, Blends and Composites: Morphology, Blends and Composites.

Kida, T., Fukuda, Y., Yamaguchi, M., Otsuki, Y., Kimura, T., Mizukawa, T., Murakami, T., Hato, K., Okawa, T., 2023. Morphological transformation of extruded isotactic polypropylene film from the Mesophase to α-form crystals. React. Funct. Polym. 191, 105682. https://doi.org/10.1016/j.reactfunctpolym.2023.105682

Kida, T., Yamaguchi, M., 2022. Role of Rigid–Amorphous chains on mechanical properties of polypropylene solid using DSC, WAXD, SAXS, and Raman spectroscopy. Polymer 249, 124834. https://doi.org/10.1016/j.polymer.2022.124834

Kilic, A., Jones, K., Shim, E., Pourdeyhimi, B., 2016. Surface crystallinity of meltspun isotactic polypropylene filaments. Macromolecular Research 24, 25-30. https://doi.org/10.1007/s13233-016-4011-y

Kim, M., Park, T.Y., Hong, S., 2021. Experimental determination of the plastic deformation and fracture behavior of polypropylene composites under various strain rates. Polym. Test. 93, 107010. https://doi.org/10.1016/j.polymertesting.2020.107010

Kim, Y.C., Ahn, W., Kim, C.Y., 1997. A study on multiple melting of isotactic polypropylene. Polym. Eng. Sci. 37, 1003-1011. https://doi.org/10.1002/pen.11745

 doi:10.20944/preprints202505.0754.v1

Kissin, Y.V., 1985. Isospecific Polymerization of Olefins With Heterogeneous Ziegler-Natta Catalysts. Springer: Berlin.

Konishi, T., Nishida, K., Kanaya, T., 2006. Crystallization of Isotactic Polypropylene from Prequenched Mesomorphic Phase. Macromolecules 39, 8035-8040. https://doi.org/10.1021/ma060191b

Konishi, T., Nishida, K., Kanaya, T., Kaji, K., 2005. Effect of Isotacticity on Formation of Mesomorphic Phase of Isotactic Polypropylene. Macromolecules 38, 8749-8754. https://doi.org/10.1021/ma050908f

Kostoski, D., Galovic, S., Suljovrujic, E., 2004. Charge trapping and dielectric relaxations of gamma irradiated radiolytically oxidized highly oriented LDPE. Radiat. Phys. Chem. 69 245-248. https://doi.org/10.1016/S0969-806X(03)00457-2

Lamberti, G., Brucato, V., 2003. Real-time orientation and crystallinity measurements during the isotactic polypropylene film-casting process. J. Polym. Sci., Part B: Polym. Phys. 41, 998-1008. https://doi.org/10.1002/polb.10411

Lanyi, F.J., Wenzke, N., Kaschta, J., Schubert, D.W., 2018. A method to reveal bulk and surface crystallinity of Polypropylene by FTIR spectroscopy - Suitable for fibers and nonwovens. Polym. Test. 71, 49-55. https://doi.org/10.1016/j.polymertesting.2018.08.018

Lanyi, F.J., Wenzke, N., Kaschta, J., Schubert, D.W., 2020. On the Determination of the Enthalpy of Fusion of α-Crystalline Isotactic Polypropylene Using Differential Scanning Calorimetry, X-Ray Diffraction, and Fourier-Transform Infrared Spectroscopy: An Old Story Revisited. Adv. Eng. Mater. 22, 1900796. https://doi.org/10.1002/adem.201900796

Laura, D.M., Keskkula, H., Barlow, J.W., Paul, D.R., 2003. Effect of rubber particle size and rubber type on the mechanical properties of glass fiber reinforced, rubber-toughened nylon 6. Polymer 44, 3347-3361. https://doi.org/10.1016/S0032-3861(03)00221-0

Lee, M., Kim, C.-H., Koo, C.-S., Kim, B.-R., Lee, Y., 2003. The variation of structure and physical properties of XLPE during thermal aging process. Polymer (Korea) 27, 249-254.

Li, J., Zhu, Z., Li, T., Peng, X., Jiang, S., Turng, L.-S., 2020. Quantification of the Young's modulus for polypropylene: Influence of initial crystallinity and service temperature. J. Appl. Polym. Sci. 137, 48581. https://doi.org/10.1002/app.48581

Li, L., Liu, T., Zhao, L., Yuan, W.-k., 2011. Effect of compressed CO2 on the melting behavior and $\beta\alpha$-recrystallization of β-form in isotactic polypropylene. The Journal of Supercritical Fluids 60, 137-143. https://doi.org/10.1016/j.supflu.2011.04.019

Li, Z., Zhou, Y., Wang, X., Liu, H., Cheng, L., Liu, W., Li, S., Guo, J., Xu, Y., 2024. Failure mechanism of metallized film capacitors under DC field superimposed AC harmonic: From equipment to material. High Voltage 9, 1081-1089. https://doi.org/10.1049/hve2.12453

Liparoti, S., Sorrentino, A., Speranza, V., 2021. Morphology-Mechanical Performance Relationship at the Micrometrical Level within Molded Polypropylene Obtained with Non-Symmetric Mold Temperature Conditioning. Polymers 13, 462. https://doi.org/10.3390/polym13030462

Liu, T.-M., Juska, T.D., Harrison, I.R., 1986. Plastic deformation of polypropylene. Polymer 27, 247-249. https://doi.org/10.1016/0032-3861(86)90333-2

Luongo, J.P., 1960. Infrared study of polypropylene. J. Appl. Polym. Sci. 3, 302-309. https://doi.org/10.1002/app.1960.070030907

Maddah, H., 2016. Polypropylene as a Promising Plastic: A Review. Am. J. Polym. Sci. 6, 1-11. https://doi.org/10.5923/j.ajps.20160601.01

Makarewicz, C., Safandowska, M., Idczak, R., Rozanski, A., 2022. Plastic Deformation of Polypropylene Studied by Positron Annihilation Lifetime Spectroscopy. Macromolecules 55, 10062-10076. https://doi.org/10.1021/acs.macromol.2c01430

Martorana, A., Piccarolo, S., Sapoundjieva, D., 1999. SAXS/WAXS study of the annealing process in quenched samples of isotactic poly(propylene). Macromol. Chem. Phys. 200, 531-540. https://doi.org/10.1002/(SICI)1521-3935(19990301)200:3<531::AID-MACP531>3.0.CO;2-K

McCrum, N.G., 1964. Density-independent relaxations in polypropylene. Journal of Polymer Science Part B: Polymer Letters 2, 495 - 498. https://doi.org/10.1002/pol.1964.110020504

 doi:10.20944/preprints202505.0754.v1

Michaeli, W., Gutberlet, D., Glißmann, M., 2001. Characterisation of the spherulite structure of polypropylene using light-microscope methods. Polym. Test. 20, 459-467. https://doi.org/10.1016/S0142-9418(00)00055-6

Mileva, D., Androsch, R., Radusch, H.-J., 2009. Effect of structure on light transmission in isotactic polypropylene and random propylene-1-butene copolymers. Polym. Bull. 62, 561-571. https://doi.org/10.1007/s00289-008-0034-7

Mileva, D., Tranchida, D., Gahleitner, M., 2018. Designing polymer crystallinity: An industrial perspective. Polymer Crystallization 1, e10009. https://doi.org/10.1002/pcr2.10009

Milicevic, D., Micic, M., Stamboliev, G., Leskovac, A., Mitric, M., Suljovrujic, E., 2012. Microstructure and crystallinity of polyolefins oriented via solid-state stretching at an elevated temperature. Fibers Polym. 13, 466-470. https://doi.org/10.1007/s12221-012-0466-4

Milicevic, D., Micic, M., Suljovrujic, E., 2014. Radiation-induced modification of dielectric relaxation spectra of polyolefins: polyethylenes vs. polypropylene. Polym. Bull. 71, 2317-2334. https://doi.org/10.1007/s00289-014-1190-6

Milicevic, D., Trifunovic, S., Galovic, S., Suljovrujic, E., 2007a. Thermal and crystallization behaviour of gamma irradiated PLLA. Radiat. Phys. Chem. 76, 1376-1380. https://doi.org/10.1016/j.radphyschem.2007.02.035

Milicevic, D., Trifunovic, S., Popovic, M., Vukasinovic-Milic, T., Suljovrujic, E., 2007b. The influence of orientation on the radiation-induced crosslinking/oxidative behavior of different PEs. Nucl. Instrum. Methods Phys. Res., Sect. B 260, 603-612. https://doi.org/10.1016/j.nimb.2007.04.157

Miller, R.L., 1960. On the existence of near-range order in isotactic polypropylenes. Polymer 1, 135-143. https://doi.org/10.1016/0032-3861(60)90021-5

Mollova, A., Androsch, R., Mileva, D., Gahleitner, M., Funari, S.S., 2013. Crystallization of isotactic polypropylene containing beta-phase nucleating agent at rapid cooling. Eur. Polym. J. 49, 1057-1065. https://doi.org/10.1016/j.eurpolymj.2013.01.015

Montanari, G.C., Fabiani D, Palmieri F, Kaempfer D, Thomann R, Mülhaupt R., 2004. Modification of electrical properties and performance of EVA and PP insulation through nanostructure by organophilic silicates. IEEE Transactions on Dielectrics and Electrical Insulation 11 754-762. https://doi.org/10.1109/TDEI.2004.1349780

Moore, E.P., 1996. Polypropylene Handbook: Polymerization, Characterization, Properties, Processing, Applications. Hanser Publishers.

Morosoff, N., Peterlin, A., 1972. Plastic deformation of polypropylene. IV. Wide-angle x-ray scattering in the neck region. Journal of Polymer Science Part A-2: Polymer Physics 10, 1237-1254. https://doi.org/10.1002/pol.1972.160100705

Na, B., Lv, R., 2007. Effect of cavitation on the plastic deformation and failure of isotactic polypropylene. J. Appl. Polym. Sci. 105, 3274-3279. https://doi.org/10.1002/app.26594

Natta, G., 1955. Une nouvelle classe de polymeres d'α-olefines ayant une régularité de structure exceptionnelle. J. Polym. Sci. 16, 143-154. https://doi.org/10.1002/pol.1955.120168205

Nitta, K.-H., 2018. Tensile Properties in β-Modified Isotactic Polypropylene, in: Wang, W., Zeng, Y. (Eds.), Polypropylene - Polymerization and Characterization of Mechanical and Thermal Properties. IntechOpen, Rijeka.

Nitta, K.-h., Odaka, K., 2009. Influence of structural organization on tensile properties in mesomorphic isotactic polypropylene. Polymer 50, 4080-4088. https://doi.org/10.1016/j.polymer.2009.06.050

Nitta, K.h., Yamaguchi, N., 2006. Influence of Morphological Factors on Tensile Properties in the Pre-yield Region of Isotactic Polypropylenes. Polym. J. 38, 122-131. https://doi.org/10.1295/polymj.38.122

Norton, D.R., Keller, A., 1985. The spherulitic and lamellar morphology of melt-crystallized isotactic polypropylene. Polymer 26, 704-716. https://doi.org/10.1016/0032-3861(85)90108-9

Olivares, N., Tiemblo, P., Gomez-Elvira, J.M., 1999. Physicochemical processes along the early stages of the thermal degradation of isotactic polypropylene I. Evolution of the γ relaxation under oxidative conditions. Polym. Degrad. Stab. 65, 297-302. https://doi.org/10.1016/S0141-3910(99)00019-1

Ozzetti, R.A., De Oliveira Filho, A.P., Schuchardt, U., Mandelli, D., 2002. Determination of tacticity in polypropylene by FTIR with multivariate calibration. J. Appl. Polym. Sci. 85, 734-745. https://doi.org/10.1002/app.10633

 doi:10.20944/preprints202505.0754.v1

Padden, F.J., Jr., Keith, H.D., 1959. Spherulitic Crystallization in Polypropylene. Journal of Applied Physics 30, 1479-1484. https://doi.org/10.1063/1.1734985

Park, J., Eom, K., Kwon, O., Woo, S., 2001. Chemical Etching Technique for the Investigation of Melt-crystallized Isotactic Polypropylene Spherulite and Lamellar Morphology by Scanning Electron Microscopy. Microscopy and microanalysis : the official journal of Microscopy Society of America, Microbeam Analysis Society, Microscopical Society of Canada 7, 276-286. https://doi.org/10.1017.s1431927601010285

Pasquini, N., 2005. Polypropylene Handbook. Carl Hanser Verlag.

Paukkeri, R., Lehtinen, A., 1993a. Thermal behaviour of polypropylene fractions: 1. Influence of tacticity and molecular weight on crystallization and melting behaviour. Polymer 34, 4075-4082. https://doi.org/10.1016/0032-3861(93)90669-2

Paukkeri, R., Lehtinen, A., 1993b. Thermal behaviour of polypropylene fractions: 2. The multiple melting peaks. Polymer 34, 4083-4088. https://doi.org/10.1016/0032-3861(93)90670-6

Pawlak, A., Rozanski, A., Galeski, A., 2013. Thermovision studies of plastic deformation and cavitation in polypropylene. Mech. Mater. 67, 104-118. https://doi.org/10.1016/j.mechmat.2013.07.016

Perepechko, I.I., 1977. Svoistva polimerov pri nizkih temperaturah. Khimiya, Moskva.

Peterlin, A., 1971. Molecular model of drawing polyethylene and polypropylene. J. Mater. Sci. 6, 490-508. https://doi.org/10.1007/BF00550305

Peterson, J.M., 1966. Thermal Initiation of Screw Dislocations in Polymer Crystal Platelets. Journal of Applied Physics 37, 4047-4050. https://doi.org/10.1063/1.1707973

Peterson, J.M., 1968. Peierls Stress for Screw Dislocations in Polyethylene. Journal of Applied Physics 39, 4920-4928. https://doi.org/10.1063/1.1655887

Pluta, M., Kryszewski, M., 1987. Studies of alpha-relaxation process in spherulitic and non-spherulitic samples of isotactic polypropylene with different molecular ordering. Acta Polym. 38, 42-52. https://doi.org/10.1002/actp.1987.010380110

Qian, C., Zhao, Y., Wang, Z., Liu, L., Wang, D., 2021. Probing the difference of crystalline modifications and structural disorder of isotactic polypropylene via high-resolution FTIR spectroscopy. Polymer 224, 123722. https://doi.org/10.1016/j.polymer.2021.123722

Qian, S., Igarashi, T., Nitta, K.-h., 2011. Thermal degradation behavior of polypropylene in the melt state: molecular weight distribution changes and chain scission mechanism. Polym. Bull. 67, 1661-1670. https://doi.org/10.1007/s00289-011-0560-6

Quijada-Garrido, I., Barrales-Rienda, J.M., Pereña, J.M., Frutos, G., 1997. Dynamic mechanical and dielectric behavior of erucamide (13-Cis-Docosenamide), isotactic poly(propylene), and their blends. J. Polym. Sci., Part B: Polym. Phys. 35, 1473-1482. https://doi.org/10.1002/(SICI)1099-0488(19970730)35:10<1473::AID-POLB1>3.0.CO;2-T

Quynn, R.G., Riley, J.L., Young, D.A., Noether, H.D., 1959. Density, crystallinity, and heptane insolubility in isotactic polypropylene. J. Appl. Polym. Sci. 2, 166-173. https://doi.org/10.1002/app.1959.070020506

Raimo, M., Silvestre, C., 2009. Topographic Analysis of Isotactic Polypropylene Spherulites by Atomic Force Microscopy. Journal of Scanning Probe Microscopy 4, 45-47. https://doi.org/10.1166/jspm.2009.1007

Read, B.E., 1990. Mechanical relaxation in isotactic polypropylene. Polymer 30, 1439-1445. https://doi.org/10.1016/0032-3861(89)90213-9

Reddy, K.R., Tashiro, K., Sakurai, T., Yamaguchi, N., Sasaki, S., Masunaga, H., Takata, M., 2009. Isothermal Crystallization Behavior of Isotactic Polypropylene H/D Blends as Viewed from Time-Resolved FTIR and Synchrotron SAXS/WAXD Measurements. Macromolecules 42, 4191-4199. https://doi.org/10.1021/ma900265u

Rodriguez-Arnold, J., Zhang, A., Cheng, S.Z.D., Lovinger, A.J., Hsieh, E.T., Chu, P., Johnson, T.W., Honnell, K.G., Geerts, R.G., Palackal, S.J., Hawley, G.R., Welch, M.B., 1994. Crystallization, melting and morphology of syndiotactic polypropylene fractions: 1. Thermodynamic properties, overall crystallization and melting. Polymer 35, 1884-1895. https://doi.org/10.1016/0032-3861(94)90978-4

Ronkay, F., Molnár, B., Nagy, D., Szarka, G., Iván, B., Kristály, F., Mertinger, V., Bocz, K., 2020. Melting temperature versus crystallinity: new way for identification and analysis of multiple endotherms of poly(ethylene terephthalate). J. Polym. Res. 27, 372. https://doi.org/10.1007/s10965-020-02327-7

 doi:10.20944/preprints202505.0754.v1

Rungswang, W., Jarumaneeroj, C., Patthamasang, S., Phiriyawirut, P., Jirasukho, P., Soontaranon, S., Rugmai, S., Hsiao, B.S., 2019. Influences of tacticity and molecular weight on crystallization kinetic and crystal morphology under isothermal crystallization: Evidence of tapering in lamellar width. Polymer 172, 41-51. https://doi.org/10.1016/j.polymer.2019.03.052

Ryan, A.J., Stanford, J.L., Bras, W., Nye, T.M.W., 1997. A synchrotron X-ray study of melting and recrystallization in isotactic polypropylene. Polymer 38, 759-768. https://doi.org/10.1016/S0032-3861(96)00583-6

Sakai, A., Tanaka, K., Fujii, Y., Nagamura, T., Kajiyama, T., 2005. Structure and thermal molecular motion at surface of semi-crystalline isotactic polypropylene films. Polymer 46, 429-437. https://doi.org/10.1016/j.polymer.2004.11.021

Schawe, J.E.K., 2017. Mobile amorphous, rigid amorphous and crystalline fractions in isotactic polypropylene during fast cooling. J. Therm. Anal. Calorim. 127, 931-937. https://doi.org/10.1007/s10973-016-5533-4

Schönherr, H., Snétivy, D., Vansco, G.J., 1993. A nanoscopic view at the spherulitic morphology of isotactic polypropylene by atomic force microscopy. Polym. Bull. 30, 567-574. https://doi.org/10.1007/BF00296476

Scoti, M., De Stefano, F., Di Girolamo, R., Malafronte, A., Talarico, G., De Rosa, C., 2023. Crystallization Behavior and Properties of Propylene/4-Methyl-1-pentene Copolymers from a Metallocene Catalyst. Macromolecules 56, 1446-1460. https://doi.org/10.1021/acs.macromol.2c02232

Séguéla, R., 2002. Dislocation approach to the plastic deformation of semicrystalline polymers: Kinetic aspects for polyethylene and polypropylene. J. Polym. Sci., Part B: Polym. Phys. 40, 593-601. https://doi.org/10.1002/polb.10118

Seguela, R., Staniek, E., Escaig, B., Fillon, B., 1999. Plastic deformation of polypropylene in relation to crystalline structure. J. Appl. Polym. Sci. 71, 1873-1885. https://doi.org/10.1002/(SICI)1097-4628(19990314)71:11<1873::AID-APP18>3.0.CO;2-I

Shang, Y., Zhao, J., Li, J., Wu, Z., Jiang, S., 2014. Investigations in annealing effects on structure and properties of β-isotactic polypropylene with X-ray synchrotron experiments. Colloid. Polym. Sci. 292, 3205-3221. https://doi.org/10.1007/s00396-014-3368-8

Sharaf, M.A., Kloczkowski, A., 2024. Evolution of the Deformation- and Flow-Induced Crystallization and Characterization of the Microstructure of a Single Spherulite, Lamella, and Chain of Isotactic Polypropylene. Macromol. Chem. Phys. 225, 2300203. https://doi.org/10.1002/macp.202300203

Shirinbayan, M., Nouira, S., Imaddahen, M.-A., Fitoussi, J., 2024. Microstructure-sensitive investigation on the plastic deformation and damage initiation of fiber-reinforced polypropylene composite. Composites Part B: Engineering 286, 111790. https://doi.org/10.1016/j.compositesb.2024.111790

Sigalas, N.I., Van Kraaij, S.A.T., Lyulin, A.V., 2023. Effect of Temperature on Flow-Induced Crystallization of Isotactic Polypropylene: A Molecular-Dynamics Study. Macromolecules 56, 8417-8427. https://doi.org/10.1021/acs.macromol.3c00916

Stachurski, Z.H., Macnicol, J., 1998. The geometry of spherulite boundaries. Polymer 39, 5717-5724. https://doi.org/10.1016/S0032-3861(97)10186-0

Starkweather, H.W., Avakian, P., Matheson, R.R., Fontanella, J.J., Wintersgill, M.C., 1992. Ultralow temperature dielectric relaxations in polyolefins. Macromolecules 25, 6871-6875. https://doi.org/10.1021/ma00051a023

Stojanović, Z., Kačarević-Popović, Z., Galović, S., Miličević, D., Suljovrujić, E., 2005. Crystallinity changes and melting behavior of the uniaxially oriented iPP exposed to high doses of gamma radiation. Polym. Degrad. Stab. 87, 279-286. https://doi.org/10.1016/j.polymdegradstab.2004.07.021

Stupp, S.I., Supan, T.J., Belton, D.J., 1979. Ice-water quenching technique for polypropylene. Orthotics and Prosthet. 33, 16-21.

Suljovrujic, E., 2000. Radiation modification of the physical properties of polyolefins. University of Belgrade, Belgrade.

Suljovrujic, E., 2002. Dielectric studies of molecular β-relaxation in low density polyethylene: the influence of drawing and ionizing radiation. Polymer 43, 5969-5978. https://doi.org/10.1016/S0032-3861(02)00505-0

Suljovrujic, E., 2005. Some aspects of structural electrophysics of irradiated polyethylenes. Polymer 46, 6353-6359. https://doi.org/10.1016/j.polymer.2005.05.113

 doi:10.20944/preprints202505.0754.v1

Suljovrujic, E., 2009a. Gel production, oxidative degradation and dielectric properties of isotactic polypropylene irradiated under various atmospheres. Polym. Degrad. Stab. 94, 521-526. https://doi.org/10.1016/j.polymdegradstab.2009.01.029

Suljovrujic, E., 2009b. The influence of molecular orientation on the crosslinking/oxidative behaviour of iPP exposed to gamma radiation. Eur. Polym. J. 45, 2068-2078. https://doi.org/10.1016/j.eurpolymj.2009.03.017

Suljovrujic, E., 2012. Complete relaxation map of polypropylene: radiation-induced modification as dielectric probe. Polym. Bull. 68, 2033-2047. https://doi.org/10.1007/s00289-012-0714-1

Suljovrujic, E., Kostoski, D., Kacarevic-Popovic, Z., Dojcilovic, J., 1999. Effect of gamma irradiation on the dielectric relaxation of uniaxially oriented low density polyethylene. Polym. Int. 48, 1193-1196. https://doi.org/10.1002/(SICI)1097-0126(199912)48:12%3C1193::AID-PI232%3E3.0.CO;2-P

Suljovrujic, E., Kostoski D, Dojcilovic J., 2001. Charge trapping in gamma irradiated low-density polyethylene. Polym. Degrad. Stab. 74, 167-170. https://doi.org/10.1016/S0141-3910(01)00150-1

Suljovrujic, E., Micic, M., Milicevic, D., 2013. Structural Changes and Dielectric Relaxation Behavior of Uniaxially Oriented High Density Polyethylene. Journal of Engineered Fibers and Fabrics 8, 155892501300800316. https://doi.org/10.1177/155892501300800316

Suljovrujic, E., Milicevic, D., Stolic, A., Dudic, D., Vasalic, D., Dzunuzovic, E., Stamboliev, G., 2024. Thermal, mechanical, and dielectric properties of radiation sterilized mesomorphic PP: Comparison between gamma and electron beam irradiation modalities. Polym. Degrad. Stab. 229, 110940. https://doi.org/10.1016/j.polymdegradstab.2024.110940

Suljovrujic, E., Stojanovic, Z., Dudic, D., Milicevic, D., 2021. Radiation, thermo-oxidative and storage induced changes in microstructure, crystallinity and dielectric properties of (un)oriented isotactic polypropylene. Polym. Degrad. Stab. 188, 109564. https://doi.org/10.1016/j.polymdegradstab.2021.109564

Suljovrujic, E., Trifunovic, S., Milicevic, D., 2010. The influence of gamma radiation on the dielectric relaxation behaviour of isotactic polypropylene. The α relaxation. Polym. Degrad. Stab. 95, 164-171. https://doi.org/10.1016/j.polymdegradstab.2009.11.034

Tadokoro, H., Kobayashi, M., Ukita, M., Yasufuku, K., Murahashi, S., Torii, T., 1965. Normal Vibrations of the Polymer Molecules of Helical Conformation. V. Isotactic Polypropylene and Its Deuteroderivatives. The Journal of Chemical Physics 42, 1432-1449. https://doi.org/10.1063/1.1696134

Tangirala, R., Baer, E., Hiltner, A., Weder, C., 2004. Photopatternable reflective films produced by nanolayer extrusion. Adv. Funct. Mater. 14, 595-604. https://doi.org/10.1002/adfm.200305446

Tarani, E., Arvanitidis, I., Christofilos, D., Bikiaris, D.N., Chrissafis, K., Vourlias, G., 2023. Calculation of the degree of crystallinity of HDPE/GNPs nanocomposites by using various experimental techniques: a comparative study. J. Mater. Sci. 58, 1621-1639. https://doi.org/10.1007/s10853-022-08125-4

Tencé-Girault, S., Lebreton, S., Bunau, O., Dang, P., Bargain, F., 2019. Simultaneous SAXS-WAXS Experiments on Semi-Crystalline Polymers: Example of PA11 and Its Brill Transition. Crystals 9, 271. https://doi.org/10.3390/cryst9050271

Teodorescu, G.M., Vuluga, Z., Ion, R.M., Fistoș, T., Ioniță, A., Slămnoiu-Teodorescu, S., Paceagiu, J., Nicolae, C.A., Gabor, A.R., Ghiurea, M., 2024. The Effect of Thermoplastic Elastomer and Fly Ash on the Properties of Polypropylene Composites with Long Glass Fibers. Polymers 16, 1238. https://doi.org/10.3390/polym16091238

Tiemblo, P., Gomez-Elvira, J.M., García Beltrán, S., Matisova-Rychla, L., Rychly, J., 2002. Melting and α relaxation effects on the kinetics of polypropylene thermooxidation in the range 80-170°C. Macromolecules 35, 5922-5926. https://doi.org/10.1021/ma0119373

Tripathi, D., 2001. Practical Guide to Polypropylene. Rapra Publishing, Shrewsbury, United Kingdom.

Umemura, T., Suzuki T, Kashiwazaki T., 1982. Impurity Effect of the Dielectric Properties of Isotactic Polypropylene. IEEE transactions on electrical insulation EI-17, 300-305.

van der Meer, D.W., 2003. Structure-Property Relationships in Isotactic Polypropylene. Twente University.

Vittoria, V., Perullo, A., 1986. Effect of quenching temperature on the structure of isotactic polypropylene films. Journal of Macromolecular Science, Part B 25, 267-281. https://doi.org/10.1080/00222348608248040

 doi:10.20944/preprints202505.0754.v1

Wang, Y., Bao, Z., Ding, S., Jia, J., Dai, Z., Li, Y., Shen, S., Chu, S., Yin, Y., Li, X., 2024. γ-Ray Irradiation Significantly Enhances Capacitive Energy Storage Performance of Polymer Dielectric Films. Adv. Mater., 2308597. https://doi.org/10.1002/adma.202308597

Wang, Y., Jiang, Z., Fu, L., Lu, Y., Men, Y., 2014. Lamellar Thickness and Stretching Temperature Dependency of Cavitation in Semicrystalline Polymers. PLoS One 9, e97234. https://doi.org/10.1371/journal.pone.0097234

Weeks, J.J., 1963. Melting Temperature and Change of Lamellar Thickness with Time for Bulk Polyethylene. Journal of research of the National Bureau of Standards. Section A, Physics and chemistry 67a, 441-451. https://doi.org/10.6028/jres.067A.046

Wunderlich, B., 1990. Thermal Analysis. Academic Press, Inc.

Yamada, K., Matsumoto, S., Tagashira, K., Hikosaka, M., 1998. Isotacticity dependence of spherulitic morphology of isotactic polypropylene. Polymer 39, 5327-5333. https://doi.org/10.1016/S0032-3861(97)10208-7

Yang, S.-G., Zhang, L.-Q., Chen, C., Cui, J., Zeng, X.-b., Liu, L., Liu, F., Ungar, G., 2023. 3D Morphology of Different Crystal Forms in β-Nucleated and Fiber-Sheared Polypropylene: α-Teardrops, α-Teeth, and β-Fans. Macromolecules 56, 5502-5511. https://doi.org/10.1021/acs.macromol.3c00788

Zhang, C., Dai, X.-Y., Xing, Z.-L., Guo, S.-W., Li, F., Chen, X., Zhou, J.-J., Li, L., 2022. Investigation on the Structure and Performance of Polypropylene Sheets and Bi-axially Oriented Polypropylene Films for Capacitors. Chin. J. Polym. Sci. 40, 1688-1696. https://doi.org/10.1007/s10118-022-2805-2

Zhang, Y.-T., Hou, S., Li, D.-L., Cao, Y.-J., Zhan, Y.-P., Jia, L., Fu, M.-l., Huang, H.-D., 2024. Hierarchical Structural Evolution, Electrical and Mechanical Performance of Polypropylene Containing Intrinsic Elastomers under Stretching and Annealing for Cable Insulation Applications. Ind. Eng. Chem. Res. 63, 11982-11991. https://doi.org/10.1021/acs.iecr.4c01348

Zhou, J.-J., Liu, J.-G., Yan, S.-K., Dong, J.-Y., Li, L., Chan, C.-M., Schultz, J.M., 2005. Atomic force microscopy study of the lamellar growth of isotactic polypropylene. Polymer 46, 4077-4087. https://doi.org/10.1016/j.polymer.2005.03.047

Zhou, Z., Ma, L., Zhen, W., Sun, X., Ren, Z., Li, H., Yan, S., 2017. An abnormal melting behavior of isotactic polypropylene spherulites grown at low temperatures. Polymer 111, 183-191. https://doi.org/10.1016/j.polymer.2017.01.052

Zhou, Z., Zhou, Q., Ren, Z., Sun, X., Li, H., Li, H., Yan, S., 2015. The αβ-iPP growth transformation of commercial-grade iPP during non-isothermal crystallization. CrystEngComm 17. https://doi.org/10.1039/C5CE01895A

Zhu, X., Yan, D., Fang, Y., 2001. In Situ FTIR Spectroscopic Study of the Conformational Change of Isotactic Polypropylene during the Crystallization Process. The Journal of Physical Chemistry B 105, 12461-12463. https://doi.org/10.1021/jp012165f

Zhuravlev, S.P., Zhuravleva NM., Polonskij Yu.A., 2002. Deformation characteristics of polypropylene film and thermal stability of capacitor insulation made on the base of polypropylene film. Elektrotekhnika 11, 36-40.

Zia, Q., Androsch, R., Radusch, H.-J., Piccarolo, S., 2006. Morphology, reorganization and stability of mesomorphic nanocrystals in isotactic polypropylene. Polymer 47, 8163-8172. https://doi.org/10.1016/j.polymer.2006.09.038

Zia, Q., Mileva, D., Androsch, R., 2008. Rigid Amorphous Fraction in Isotactic Polypropylene. Macromolecules 41, 8095-8102. https://doi.org/10.1021/ma801455m

Zia, Q., Radusch, H.-J., Androsch, R., 2009. Deformation behavior of isotactic polypropylene crystallized via a mesophase. Polym. Bull. 63, 755-771. https://doi.org/10.1007/s00289-009-0151-y

Zuo, F., Keum, J.K., Chen, X., Hsiao, B.S., Chen, H., Lai, S.-Y., Wevers, R., Li, J., 2007. The role of interlamellar chain entanglement in deformation-induced structure changes during uniaxial stretching of isotactic polypropylene. Polymer 48, 6867-6880. https://doi.org/10.1016/j.polymer.2007.08.065